DR. DEBJANI SIHI (Orcid ID : 0000-0002-5513-8862)

DR. KATHLEEN SAVAGE (Orcid ID : 0000-0002-1649-5314)

Article type : Primary Research Articles

Title: Simultaneous numerical representation of soil microsite production and consumption of carbon dioxide, methane, and nitrous oxide using probability distribution functions

Running Title: Soil microsites affect greenhouse gas fluxes

Debjani Sihi[1, 2]*, Eric A. Davidson[1], Kathleen E. Savage[3], and Dong Liang[4]

[1]University of Maryland Center for Environmental Science, Appalachian Laboratory, 301 Braddock Road, Frostburg, MD 21532, USA. [2] Now at Climate Change Science Institute, Environmental Sciences Division, Oak Ridge National Laboratory, 1 Bethel Valley Rd, Oak Ridge, TN-37830, USA, [3]Woods Hole Research Center, 149 Woods Hole Road, Falmouth, MA 02540, USA, [4]University of Maryland Center for Environmental Science, Chesapeake Biological Laboratory, 146 Williams Street, Solomons, MD 20688, USA.

*Corresponding author (telephone: 865-574-9166, *email: sihid@ornl.gov*, *darisihi@gmail.com*)

Abstract

Production and consumption of nitrous oxide (N_2O), methane (CH_4), and carbon dioxide (CO_2) are affected by complex interactions of temperature, moisture, and substrate supply, which are further complicated by spatial heterogeneity of the soil matrix. This microsite heterogeneity is often invoked to explain non-normal distributions of greenhouse gas (GHG) fluxes, also known as hot spots and hot moments. To advance numerical simulation of these belowground processes, we expanded the Dual Arrhenius and Michaelis-Menten (DAMM) model, to apply it consistently for all three GHGs with respect to the biophysical processes of production, consumption, and diffusion within the soil, including the contrasting effects of oxygen (O_2) as substrate or inhibitor for each process. High-frequency chamber-based measurements of all three GHGs at the Howland Forest (ME, USA) were used to parameterize the model using a multiple constraint approach. The area under a soil chamber is partitioned according to a bivariate lognormal probability distribution function (PDF) of carbon (C) and water content across a range of microsites, which leads to a PDF of heterotrophic respiration and O_2 consumption among microsites. Linking microsite consumption of O_2 with a diffusion model generates a broad range of microsite concentrations of O_2, which then determines the PDF of microsites that produce or consume CH_4 and N_2O, such that a range of microsites occurs with both positive and negative signs for net CH_4 and N_2O flux. Results demonstrate that it is numerically feasible for microsites of N_2O reduction and CH_4 oxidation to co-occur under a single chamber, thus explaining occasional measurement of simultaneous uptake of both gases. Simultaneous simulation of all three GHGs in a parsimonious modeling framework is challenging, but it increases confidence that agreement between simulations and measurements is based on skillful numerical representation of processes across a heterogeneous environment.

Keywords: soil microsite, probability distribution function, greenhouse gas, CO_2, CH_4, N_2O, DAMM, DAMM-GHG

Introduction

Fluxes of greenhouse gases (GHGs) from soil to the atmosphere are likely to play a significant role as biotic feedbacks to climate change (Ciais et al., 2013; Davidson and Janssens, 2006). Soils under forest, agriculture, and other land-use classes contribute to nearly a quarter of global emissions of GHGs, including carbon dioxide (CO_2), methane (CH_4), and nitrous oxide (N_2O) (IPCC, 2014). Production and consumption of these biogenic GHGs are often associated with complex processes, involving carbon (C), nitrogen (N), and oxygen (O_2) substrates and inhibitors, and environmental controllers such as temperature, moisture, and transport of solutes and gases (Conrad, 1996), which remain challenging to simulate in ecosystem and Earth system models (ESMs).

In this special issue, we present an expansion of a numerical soil process model that is a logical progression of several papers published by our group in the pages of this journal. While the importance of temperature on soil heterotrophic activity has been recognized for over a century (Arrhenius, 1889; Lloyd & Taylor, 1994; Van't Hoff, 1898), and optima at intermediate values of soil moisture have also been well described (Hursh et al. 2017; Linn & Doran, 1984; Moyano et al., 2013), empirical relationships with these driving factors have had limited value in revealing a mechanistic understanding of soil respiration. Davidson et al. (1998) demonstrated that soil temperature and moisture had opposite seasonal trends in a moist temperate forest, resulting in confounding effects on soil respiration. Drawing on a growing body of research on soil respiration in the 1990s and 2000s, Davidson et al. (2006) reviewed the emerging recognized need to move beyond mostly temperature functions, such as Q_{10}s, and to mechanistically link temperature and moisture drivers to substrate supply for soil heterotrophic respiration. Those concepts formed the basis of a parsimonious numerical model that used Dual Arrhenius and Michaelis-Menten (DAMM) kinetics to link soil temperature and moisture to their effects on substrate supply for soil respiration (Davidson et al., 2012). In the 20-year special issue of this journal, Davidson et al. (2014) described a vision for how the DAMM model could be conceptually linked to related processes of soil carbon dynamics, which has since been demonstrated in the modular Millennial Model (Abramoff et al., 2018), and how it could be integrated into large ecosystem models, which was since demonstrated by Sihi et al. (2018). Davidson et al. (2014) also proposed that other soil trace gas emissions could be simulated using the DAMM approach.

Here we offer a new version of DAMM for the greenhouse gases, CO_2, CH_4, and N_2O (hereafter, DAMM-GHG: Dual Arrhenius and Michaelis Menten-Greenhouse Gas). We use three simultaneous data streams from chamber measurements of CO_2, CH_4, and N_2O fluxes in a New England forest to constrain the DAMM-GHG model, which has a common structure for biophysical processes of production, consumption, and diffusion within the soil, including the contrasting effects of oxygen (O_2) as substrate or inhibitor for each process. Another innovation presented here is to represent soil microsite heterogeneity of soil carbon and moisture contents with probability distribution functions (PDFs) and to simulate the production and consumption of each gas at a microsite scale, rather than the traditional modeling approach of using bulk soil means of measured carbon and moisture as model drivers.

Thermodynamic theories suggest that CH_4 oxidation (aka methanotrophy) should proceed under aerobic conditions and CH_4 production (aka methanogenesis) should be favored under anaerobic (or reducing) conditions (Conrad, 2009; Dean et al., 2018). Production of N_2O via nitrification and denitrification processes are known to peak at an optimal intermediate soil moisture content, whereas, reducing soil conditions under high water content are thought to be prerequisites for N_2O reduction to N_2 via classical denitrification (Davidson, 1991; Butterbach-Bahl et al., 2013; Firestone & Davidson, 1989). While a large body of literature generally supports these patterns, there are exceptions that are frequently attributed to spatial heterogeneity within soils and soil microsites.

While the highest rates of net consumption of atmospheric N_2O (i.e. N_2O reduction) is observed in wetlands, N_2O reduction in well-drained upland soils has been observed sporadically for many years (Chapuis-Lardy et al., 2007; Schlesinger, 2013; Syakila & Kroeze, 2010). Such observations have often been discounted as measurement error or noise. The recent advent of fast response field instruments with good sensitivity and precision has permitted confirmation that upland soils can be small sinks of N_2O (Eugster et al., 2007; Savage et al., 2014), and a modest soil sink for atmospheric N_2O is now generally accepted as plausible for some sites and times. Increasing soil sink strength of N_2O during drought events further increases perplexity, given that drought events generally facilitate soil aeration (Goldberg & Gebauer, 2009). Occasional observations of net emissions of CH_4 from well-drained upland soils, although contrary to expectations, are also common (Brewer et al., 2018; Cattânio et al., 2002; Keller & Matson, 1994; Silver et al., 1999; Teh et al., 2005; Verchot et al., 2000).

Spatial heterogeneity of soil microsites is often invoked to explain net atmospheric uptake of N_2O and net emissions of CH_4 from well-drained upland soils. Soil heterogeneity at micro-scales can cause a wide range of microsite redox potentials and concentrations of substrates, which must be accounted for to explain highly skewed distributions of soil GHG fluxes (Parkin, 1987, 1993; Savage et al., 2014; Stoyan et al., 2000). Because existing ESMs are not able to represent the underlying mechanisms that control variation in enzymatic processes at microsite scales (Tian et al., 2019; Xu et al., 2016), these models often fail to capture the dynamics of soil GHG fluxes, including the so-called hot-spots and hot-moments (Groffman, 2009; Groffman, 2012; Lurndahl, 2016; Saha et al., 2018) or control points (Bernhardt et al., 2017).

Only recently have modeling activities at ecosystem (or landscape) scales begun to shift from the classical framework based on redox strata (or water table position) and mean measured soil moisture to emerging conceptual frameworks that consider heterogeneous environment for production and consumption of GHGs (Ebrahimi & Or, 2018; Or, 2019; Keiluweit et al., 2018; Wang et al., 2019; Yang et al., 2017). However, to our knowledge, mechanistic simulation of simultaneous production, consumption, and diffusion of multiple gases (CO_2, CH_4, N_2O, and O_2) among multiple soil microsites has not yet been attempted. Numerical representation of microsite production and consumption of multiple GHGs is necessary to simulate concurrent N_2O reduction and CH_4 oxidation processes in well-drained upland soils (Savage et al., 2014). The overall objective of this work is to demonstrate that the qualitative explanations of microsite heterogeneity can be expressed in a mathematically consistent biophysical process model that is numerically consistent with simultaneously measured fluxes of all three GHGs: CO_2, CH_4, and N_2O.

While originally developed for aerobic heterotrophic respiration (i.e. Rh), here we expand the original core structure of the DAMM model (Davidson et al., 2012, 2014; Fig. S1) to represent methanogenesis, methanotrophy, N_2O production, and N_2O reduction reactions using the same framework and physics for simulating the availability of O_2 and other substrates and for diffusion of gases across soil-atmosphere boundary using microsite PDFs (Figs. 1, S1). Simultaneously constraining our GHG enzyme kinetic model (i.e. DAMM-GHG) with observations of fluxes of multiple GHGs presents large challenges, because tuning a model to agree with one data stream may cause a poorer fit to a second or third data stream. However, if all data streams can be simultaneously simulated with adequate fidelity and skill, this multiple constraint approach enhances the probability that the parameterization and process representations are realistic and robust. One can never be certain that a model gets the “right answer for the right reason,” but challenging a single model with multiple data streams of related but differing processes, such as CO_2, CH_4, and N_2O fluxes, confers additional credence to its structure and parameterization.

Materials and Methods

Site Description and Data Collection

We measured GHG fluxes in a mature boreal-transition forest with a hummock-hollow microtopography, Howland Forest research site (45.20°N, 68.74°W) from central Maine, USA. Mean annual temperature and mean annual precipitation are +5.5 °C and 1000 mm, respectively. Soils of the Howland Forest upland sites are characterized as Skerry fine sandy loam, frigid Aquic Haplorthods. More information on the Howland Forest research site can be found in Fernandez et al. (1993).

High frequency (sampling frequency: 1 Hz) real-time soil CH_4 and N_2O fluxes were measured using an Aerodyne quantum cascade laser (QCL) integrated with soil CO_2 flux measurements by LI-COR IRGA assembly. Triplicate chambers were each sampled once every two hours. Chamber tops were closed for 5 minutes and automated fluxes were calculated by fitting a linear regression on the change in headspace GHG concentrations followed by temperature and pressure corrections. We characterized the uncertainty of measurements by the standard deviation estimates for all three GHGs. Soil temperature and soil moisture were measured at each chamber location at 10 cm depth once every hour using a Type-T thermocouple and Campbell Scientific CS616 water content reflectometer probes, respectively and stored on a Campbell Scientific CR10X data-logger (Campbell Scientific, Logan, UT). We used daily average values of both drivers (soil temperature and soil moisture) and GHG fluxes for modeling purposes to smooth high measurement noise observed at sub-daily time scale. See Savage and Davidson (2003) for more details on our chamber design and automated sampling system. Quality control protocols for soil GHG fluxes can be found in Savage et al. (2008, 2014).

Modeling Scheme

Aerobic and anaerobic processes in soil are linked through heterotrophic dependence on fixed C sources for energy, but with contrasting effects of O_2 as either essential substrate or potential inhibitor (Figs. 1, S1). To date, most biogeochemical models use separate model versions for simulating soil organic matter decomposition resulting in CO_2 emissions and the processes affecting CH_4 and N_2O emissions, but here we simultaneously simulate biogeochemically linked multiple GHG emissions using the same biophysical framework.

For the present study, we focus primarily on heterotrophic respiration being the dominant source of CO_2 production and fate of O_2 consumption, with the resulting O_2 concentrations then affecting the net fluxes of CH_4 and N_2O by methanogenesis, methanotrophy, nitrification, and denitrification processes. The logic for coupled simulation of CO_2, CH_4, and N_2O fluxes in the DAMM-GHG model, illustrated in Fig. 1, is as follows:

1. The measured soil C and soil moisture can be partitioned according to a simulated log-normal PDF, such as a distribution where only a small fraction of microsites has high soil C or high soil moisture.
2. Log-normal PDFs of soil C-substrates and soil moisture among microsites lead to a simulated PDF of heterotrophic respiration (Rh), applying the original DAMM model independently to each microsite within the PDF.
3. Simulated microsite CO_2 production is aggregated to the chamber scale to estimate heterotrophic respiration contributing to the chamber flux measurement. We then estimate the total soil CO_2 flux by adding the contribution of root-derived CO_2 fluxes to Rh based on previously measured ratios at the Howland Forest (Carbone et al., 2016; Savage et al., 2018; Sihi et al., 2018). A distinct seasonal pattern of the contribution of root-derived CO_2 (Ra) to total soil CO_2 fluxes (SR) increased from 0.50 in early spring to around 0.65 in early autumn, followed by a declining trend through winter (Fig. S2). Total chamber-based measurements of CO_2 efflux are used as a constraint for the sum of the simulated root and heterotrophic CO_2 production rates across the simulated PDF of microsites.
4. The simulated and measured soil CO_2 efflux is a reasonable proxy for O_2 demand within the soil. The respiration quotient is not exactly unity, but is usually close enough to unity in non-calcareous soils to allow simulation of O_2 consumption within the soil based on measurement-constrained simulated CO_2 efflux (Angert et al., 2015). Knowledge of respiration quotient would be needed for the application of our DAMM-GHG model to calcareous soils. We

assumed that the simulation of O_2 consumption by the original version of the DAMM model serves our purpose of estimating the O_2 demand (or consumption) here (see Fig. S1).

5. Microsite PDFs of O_2 concentrations are then simulated as a function of O_2 consumption rates distributed across microsites and gaseous diffusion rates using the same DAMM functions in Fig. S1 driven by air-filled porosity.
6. Next, the resulting PDF of O_2 concentrations is used to simulate methanogenesis, methanotrophy, N_2O production, and N_2O consumption at the scale of each of the distributed microsites according to similar Michaelis-Menten and diffusion equations (Fig. S1), where O_2 serves as either inhibitor or substrate (Davidson et al., 2014). The net CH_4 and N_2O flux summed across simulated PDFs of microsites are constrained by observed chamber-based fluxes of CH_4 and N_2O.

We used soluble C as a proxy for the reducing power needed for methanogenesis. However, future studies may explicitly represent specific substrates for acetoclastic and hydrogenotrophic methanogenic pathways, if parameterization of that type of model structure can be constrained by the availability of data on concentrations of organic acids (acetate, formate) and hydrogen (H_2), which was not the case for our study. We also assumed that respiration is the dominant pathway of CO_2 production in soil. Thus, we did not account for the minor contribution of acetoclastic methanogens to CO_2 production and hydrogenotrophic methanogens to CO_2 consumption. Likewise, we considered soil respiration is the major sink of O_2 and ignored the otherwise small fraction of O_2 consumed by methanotrophs.

We added a nitrification module to account for the N_2O production during nitrification using the observed seasonal dynamics of ammonium (NH_4^+) in our study area (Fernandez et al., 1995). The Howland Forest is a strongly nitrogen-limited system, with porewater nitrate (NO_3^-) concentration always close to detection limits by inductively coupled plasma-mass spectrometry, ICP-MS (Fernandez et al., 1995). N_2O production during classical denitrification is mechanistically simulated using seasonally averaged porewater NO_3^- data along-with microsite PDFs of soil C and soil moisture. Nitrous oxide is reduced to N_2 during classical denitrification following the Hole-in-the-Pipe conceptual model, including possible reduction of atmospheric N_2O that diffuses into the soil (Firestone & Davidson, 1989). See supplementary material (section S2) for DAMM-GHG model equations.

Microsite Probability Distribution Functions of Soil C and Soil Moisture

The microsite PDFs of soil C substrate and soil moisture were generated from a bivariate truncated log-normal distribution. The PDF for soil C was truncated at 0.001 and 0.15 (g cm^{-3}), respectively. The soil C PDF was distributed with mean equaling the observed soil C value (see Fig. S3 for more information on the PDF of soil C). Likewise, the soil moisture PDF was distributed with mean equaling the observed soil moisture value, truncations at 70% and 200% of the observed mean soil moisture values. The spatial heterogeneity of soil C and soil moisture were constrained by optimizing the parameters (standard deviation and/or coefficient of variation) that control the skewness of soil C and soil moisture PDFs by enveloping the bounds reported by Stoyan et al. (2000). If the upper truncation limit of the soil moisture PDF exceeded the soil pore volume, we reset it to 95% of the porosity value. We constructed the microsite PDF as the product of two lognormal distributions of soil C and soil moisture. The PDF was evaluated at 10 × 10 equally spaced quantiles for soil C and soil moisture, respectively.

Here we focused on spatial heterogeneity across soil microsites at the mm and sub-mm scale. Within stand heterogeneity at the meter scale, such as variation in bulk density and porosity along topographical gradients, is not account for in this study.

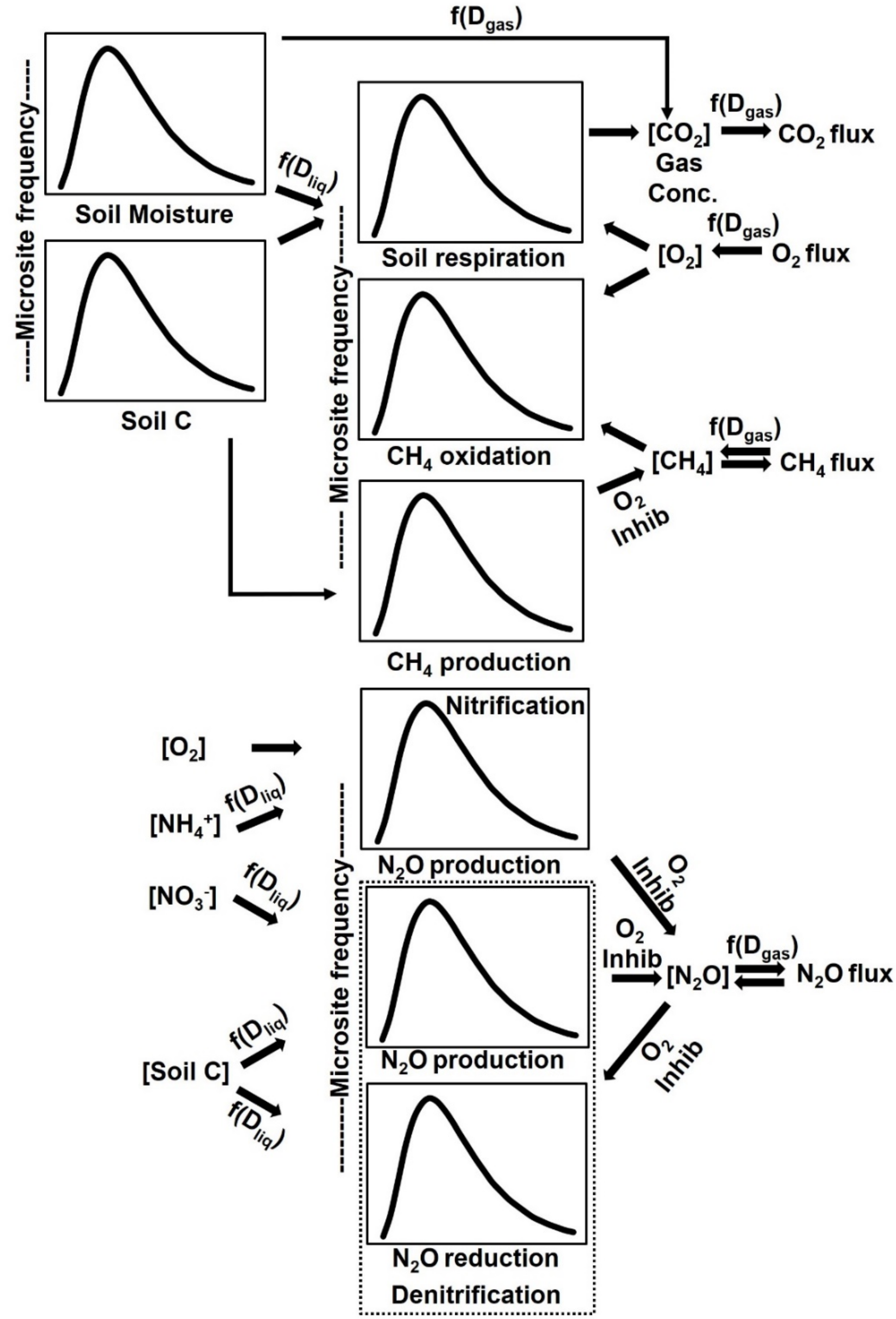

Fig. 1: Conceptual framework for simultaneous representation of CO_2, CH_4, and N_2O fluxes in DAMM-GHG model. Inhib represent inhibition. f(D_{gas}) and f(D_{liq}) represent soil moisture effect on diffusion of gases and soluble substrates, respectively.

Parameter Optimization and Uncertainty Analysis

We optimized model parameters within a Bayesian Markov chain Monte Carlo (MCMC) framework (see section S1 for more details on the optimization algorithm). We implemented the MCMC algorithm using *mcmc* and *doParallel* packages (Revolution Analytics & Weston, 2015) in the R (version 3.3.2) statistical programming language (R Core Team, 2018). We applied a posterior predictive procedure to estimate the uncertainty of the optimized parameters. We implemented the posterior predictive analyses using the *R-INLA* package (Lindgren & Rue, 2015; Rue et al., 2009). We divided daily-average soil GHG flux measurements into alternative synoptic-scale periods of 10 days, where we used one-half of measured GHG fluxes for model calibration and another half for model validation.

Sensitivity Analysis

We evaluated the sensitivity of model parameters using a global variance-based sensitivity analysis and a collinearity (or parameter identifiability) analysis. We implemented a variance-based sensitivity analysis using the R-*multisensi* package, where a generalized sensitivity index (ranging between 0 to 1, extracted from the first axis of principle component analysis) was used to determine the sensitivity of multiple GHG fluxes to each model parameter value (Bidot et al., 2018). The global sensitivity analysis quantifies the proportion of variability accounted by each of the parameters on model outputs, where a high GSI value indicates that the simulation results are highly sensitive to that parameter (Lamboni et al., 2009).

We implemented the collinearity analysis using the *collin* function of *R-FME* package, where the collinearity index (CI) was used to determine the linear dependence of model parameters to each other (Brun et al., 2001; Soetaert & Petzoldt, 2010; Soetaert, 2016). In general, higher values of CI indicate increased equifinality (or decreased number of identifiable parameters) of model parameters. One can compensate $(1 - \frac{1}{\mathrm{CI}})$ % of the effect of a change in one parameter by modifying the values of other parameters. Hence, CI values can range between 1 (when all terms are orthogonal or all subsets of parameters are identifiable) to infinity (when all terms are linearly dependent, or no single subset of parameters is identifiable). The CI value of 15 is considered as a threshold above which approximate linear dependence of model parameters increases and poor identifiability can be expected (*sensu* Omlin et al., 2001).

Results

Seasonality of Soil Greenhouse Gas Fluxes

Soil CO_2 fluxes followed the typical seasonal trend of soil temperature, where both seasonal average and peak CO_2 fluxes were comparable between 2015 (average (min-max): 171 (73-297) mg CO_2-C m^{-2} hr^{-1}) and 2016 (average (min-max) measurement period: 168 (52-281) mg CO_2-C m^{-2} hr^{-1}) (Fig. 2). This is due, in part, to the comparable seasonal soil temperature ranges between 2015 (average:14.4 °C, ranged between 8.4 to 18.6 °C) and 2016 (average: 13.3 °C, ranged between 5.6 to 17.9 °C) measurement periods (Figs. 2, 3). Soil CO_2 fluxes exponentially increased with soil temperature (R^2 = 0.75) (Fig. 3a). We also observed a typical bell-shaped relationship between CO_2 flux and soil moisture (R^2 = 0.16), with the optimum for CO_2 flux at intermediate water contents (Fig. 3d). Although the effect of soil moisture on CO_2 fluxes was always secondary to soil temperature (Fig. S5), the fit with soil moisture was better when it was more limiting in the dry summer of 2016 than the wet summer of 2015 (R^2 = 0.24 and 0.52 in 2015 and 2016, respectively) (Fig. S6d).

In contrast to CO_2 fluxes, soil CH_4 fluxes mimicked the seasonal trend of soil moisture for both years (Fig. 2b,g). Soil moisture and net CH_4 fluxes were positively related (R^2 = 0.70), although the slope of the linear regression line was steeper during 2016 than during 2015 (Figs. 3e, S6e). We observed relatively smaller net CH_4 oxidation in the spring followed by higher net CH_4 oxidation in summer months, and again lower net CH_4 oxidation in the autumn. Although seasonal average values were generally similar, the range of CH_4 flux values in 2016 (average: -0.07 μg CH_4-C m^{-2} hr^{-1}, min-max range: -0.13 to 0.004 μg CH_4-C m^{-2} hr^{-1}) was wider than in 2015 (average: -0.05 μg CH_4-C m^{-2} hr^{-1}, min-max range: -0.08 to -0.03 μg CH_4-C m^{-2} hr^{-1}).

Unlike CO_2 and CH_4, the seasonal trend of soil N_2O fluxes contrasted between 2015 vs. 2016 (Figs. 2c,h, 3f, S6f). The 2015 growing season was significantly wetter than the 2016 growing season. The cumulative precipitation of the summer months (June 1 to Sept 30) of 2015 and 2016 was 439 mm and 279 mm, respectively (source: https://www.ncdc.noaa.gov/crn/). Consequently, the average soil moisture was generally higher (24.8 v v^{-1}, min-max range: 14.8 to 32.6 v v^{-1}) during the 2015 growing season (measured over June 11 to Oct 17) than the average soil moisture (19.7 v v^{-1}, min-max range: 8.9 to 27 v v^{-1}) during the 2016 growing season (measured over May 3 to Nov 6) (Figs. 2d,i, 3f, S6f).

We observed low rates of net N_2O consumption during the spring of 2015 when soil moisture was highest, which was followed by mostly near zero net emissions and a few positive emissions throughout the 2015 summer (Fig. 2c,d). In contrast, we observed net positive N_2O emission during the early spring of 2016 and net N_2O consumption throughout most of the 2016 growing season, when soil moisture was minimal (Fig. 2h,i). The temperature effect was weak and inconsistent between two years (Figs. 3c, S6c). On average, we observed small net N_2O emission during the 2015 growing season (average: 0.06 µg N_2O-N m^{-2} hr^{-1}, ranged between -0.77 to 1.73 µg N_2O-N m^{-2} hr^{-1}) and net N_2O consumption during the 2016 growing season (average: -0.18 µg N_2O-N m^{-2} hr^{-1}, ranged between -1.10 to 1.68 µg N_2O-N m^{-2} hr^{-1}).

Performance of the DAMM-GHG Model

Overall, the model reproduced the seasonal dynamics of soil greenhouse gas fluxes (Figs. 2, 4). The model explained 72% of the variation in soil CO_2 fluxes (Fig. 4a). Likewise, the 1:1 relation between the observed and simulated soil CH_4 fluxes was remarkable (R^2 = 0.78) (Fig. 4b). The model marginally overestimated CO_2 fluxes and underestimated CH_4 fluxes during early spring of 2016 (Fig. 2f,g).

Soil N_2O fluxes were relatively noisier as compared to CO_2 and CH_4 fluxes with a few outliers in both years (red triangles and squares in Fig. 2 and 4, respectively). The model generally explained the dynamics of N_2O fluxes (R^2 = 0.36 and 0.52 with and without outliers, respectively) (Fig. 4c). The model did not capture the few very low net N_2O fluxes observed in the peak season of 2016. Most importantly, the model captured the instances when net atmospheric consumption of CH_4 (i.e. net CH_4 oxidation) co-occurred with net atmospheric consumption of N_2O (i.e. net N_2O reduction) within the same soil chamber and at two extremes of the measured soil moisture, during the early wet spring of 2015 and during the driest period of the 2016 growing season (see Fig. 2c,h and red circles in Fig. 3f).

In general, there was little bias in the relations between the observed and simulated GHG fluxes (slope ranged between 0.98 to 1.10) (Fig. 4). The 95% CI of the simulated GHGs for all, CO_2, CH_4, and N_2O, were narrow and the model parameter values were generally well-constrained. The interquartile ranges in the posterior distributions of all parameters were less than half of their respective prior interquartile ranges (Table 1). The prior interquartile ranges represent the approximate upper and lower bounds of the measured values from the relevant literature.

The effective depth in the DAMM-GHG model was optimized to a median value of 7 cm (min-max range: 6-11 cm; Table 1), indicating that most of the important processes affecting the net GHG fluxes that we measured with chambers were occurring within the topsoil horizons at this site. The number of microsites within the 0.07 m^2 chamber footprint was optimized to a median value of 7000 (min-max range: 2000-9000; Table 1), indicating that the simulated microsites were about 3.6 mm in diameter, which could include macroaggregates and clusters of fine roots and pockets of organic debris.

Sensitivity Analysis

Soil moisture primarily (and soil temperature secondarily) controlled the microsite PDFs of production, consumption, and diffusion processes of CO_2, CH_4, and N_2O. The net flux is the net effect of production, consumption, and diffusion of individual gases (Figs. 5, S10). Of all parameters, the most sensitive ones were those that control the Vmax terms in the Arrhenius equation (Ea and α) for production and consumption of individual GHGs, followed by the half-saturation constants (Km's) and O_2 inhibition coefficients (KI's) for each process (Fig. 6). The linear dependence of the DAMM-GHG model parameters was generally low and was usually below the threshold of 15 (with a few exceptions) identified for potential equifinality issues (Fig. 7).

Table1: Parameters used for simultaneous simulation all three greenhouse gases in the DAMM-GHG model.

Parameter	Description	Unit	Prior range	Posterior range	Source
For CO_2 module					
α_{CO_2}	Base rate for soil respiration	µmole CO_2 L^{-1} hr^{-1}	$2*10^{10}(2*10^{9}, 2*10^{11})$	$5*10^{9}(2*10^{9}, 9*10^{9})$	Abramoff et al., 2017 Davidson et al., 2012 Sihi et al., 2018
Ea_{CO_2}	Temperature sensitivity for soil respiration	kJ mol^{-1}	72(60,80)	66(64-72)	
kM_{C-CO_2}	Half-saturation constant of C for soil respiration	µmole C L^{-1}	1(0.1,100)	0.9(0.7,1.6)	
$kM_{O_2-CO_2}$	Half-saturation constant of O_2 for soil respiration	µmole O_2 L^{-1}	100(3,300)	16(4,38)	
Depth	Effective depth	cm	15(5,30)	7(6,11)	This study
Total microsite	Total number of microsites	unitless	$10^{4}(10^{3},10^{5})$	$7*10^{3}$ $(2*10^{3}, 9*10^{3})$	This study
Soil C_{SD}	Coefficient that determine skewness of soil carbon PDF	unitless	0.5(0.1,0.9)	0.5(0.1,0.9)	Stoyan et al., 2000
Soil $Moisture_{SD}$	Coefficient that determine skewness of soil moisture PDF	%	20(5,30)	7(6-12)	Stoyan et al., 2000

For CH_4 module					
α_{CH_4prod}	Base rate for CH_4 production	µmole CH_4 L^{-1} hr^{-1}	$3*10^5(3*10^4,3*10^6)$	$3*10^5(2*10^5,6*10^5)$	This study
Ea_{CH_4prod}	Temperature sensitivity for CH_4 production	kJ mol^{-1}	100(50,150)	74(68,78)	Nedwell & Watson, 1995 Westermann, 1993
kM_{C-CH_4}	Half-saturation constant of C for CH_4 production	µmole C L^{-1}	1(0.1-100)	1.2(0.9,2.1)	This study
kI_{CH_4}	Inhibition coefficient of O_2 for CH_4 production	µmole O_2 L^{-1}	3(0.3-4.3)	0.43(0.4,0.9)	Arah & Stephen, 1998
α_{CH_4ox}	Base rate for CH_4 oxidation	µmole CH_4 L^{-1} hr^{-1}	0.07(0.007,7)	0.1(0.08,2)	Davidson et al., 2014
Ea_{CH_4ox}	Temperature sensitivity for CH_4 oxidation	kJ mol^{-1}	30(10,50)	34(32,37)	Crill et al., 1994
kM_{CH_4}	Half-saturation constant of CH_4 for CH_4 oxidation	µmole CH_4 L^{-1}	$10^{-2}(10^{-3},10^{-1})$	0.005(0.002,0.006)	Davidson et al., 2014
$kM_{O_2-CH_4}$	Half-saturation constant of O_2 for CH_4 oxidation	µmole O_2 L^{-1}	43(3,300)	24(13,33)	Davidson et al., 2014
For N_2O module					

$\alpha_{N_2O_{prod-nitrif}}$	Base rate for nitrification	µmole N_2O L^{-1}	$10^2(10^1,10^3)$	282(207,722)	This study
$Ea_{N_2O_{prod-nitrif}}$	Temperature sensitivity for N_2O production during nitrification	kJ mol^{-1}	60(45,75)	62(57,67)	Stark, 1996 Stark & Firestone, 1996
kM_{NH_4}	Half-saturation constant of NH_4^+ for N_2O production	µmole NH_4^+ L^{-1}	15 (8,22)	9(8,10)	Stark & Firestone, 1996 Zarnetske et al., 2012
$kM_{O_2-N_2O}$	Half-saturation constant of O_2 for N_2O production	µmole O_2 L^{-1}	100(9,163)	36(15,44)	Bodelier et al., 1996 Veresetre & Focht, 1977 Zarnetske et al., 2012
$\alpha_{N_2O_{prod-denitrif}}$	Base rate for N_2O production	µmole N_2O L^{-1}	$10^2(10^1,10^3)$	520(438,958)	This study
$Ea_{N_2O_{prod-denitrif}}$	Temperature sensitivity for N_2O production during denitrification	kJ mol^{-1}	60(45,75)	67(65,71)	Canion et al., 2014 Holtan-Hartwig et al., 2000 Vieten, 2008
kM_{NO_3}	Half-saturation constant of NO_3^- for N_2O production	µmole NO_3^- L^{-1}	26(15,57)	17(16,19)	Zarnetske et al., 2012

$kI_{N_2O-prod}$	Inhibition coefficient of O_2 for N_2O production	µmole O_2 L^{-1}	14.3(4.3,43)	41(40,42)	Körner & Zumft, 1989 Zarnetske et al., 2012
kM_{C-N_2O}	Half-saturation constant of C for N_2O production and reduction during denitrification	µmole C L^{-1}	1(0.1-100)	0.6(0.3,1)	This study
$\alpha_{N_2O_{red}}$	Maximum velocity for N_2O reduction	µmole N_2O L^{-1}	$10^3(10^2,10^4)$	3413(1585,9583)	This study
$Ea_{N_2O_{red}}$	Temperature sensitivity for N_2O reduction	kJ mol^{-1}	50(45,75)	47(46,47)	Canion et al., 2014 Holtan-Hartwig et al. (2000) Vieten, 2008
kM_{N_2O}	Half-saturation constant of N_2O for N_2O reduction	µmole N_2O L^{-1}	0.16(0.05,0.27)	0.19(0.13,0.26)	Holtan-Hartwig et al., 2000 Vieten, 2008
kI_{N_2O-red}	Inhibition coefficient of O_2 for N_2O reduction	µmole O_2 L^{-1}	7.5(4.3,20.1)	19.5(18.6,19.7)	Körner & Zumft, 1989 Vieten., 2008

PDF: Microsite probability distribution function. Prior range represents initial (min-max) of prior interquartile range. Posterior range represents median (95% CI) of posterior interquartile range. Units for all base rates, i.e. α(s), are in µmole concentration dissolved in water.

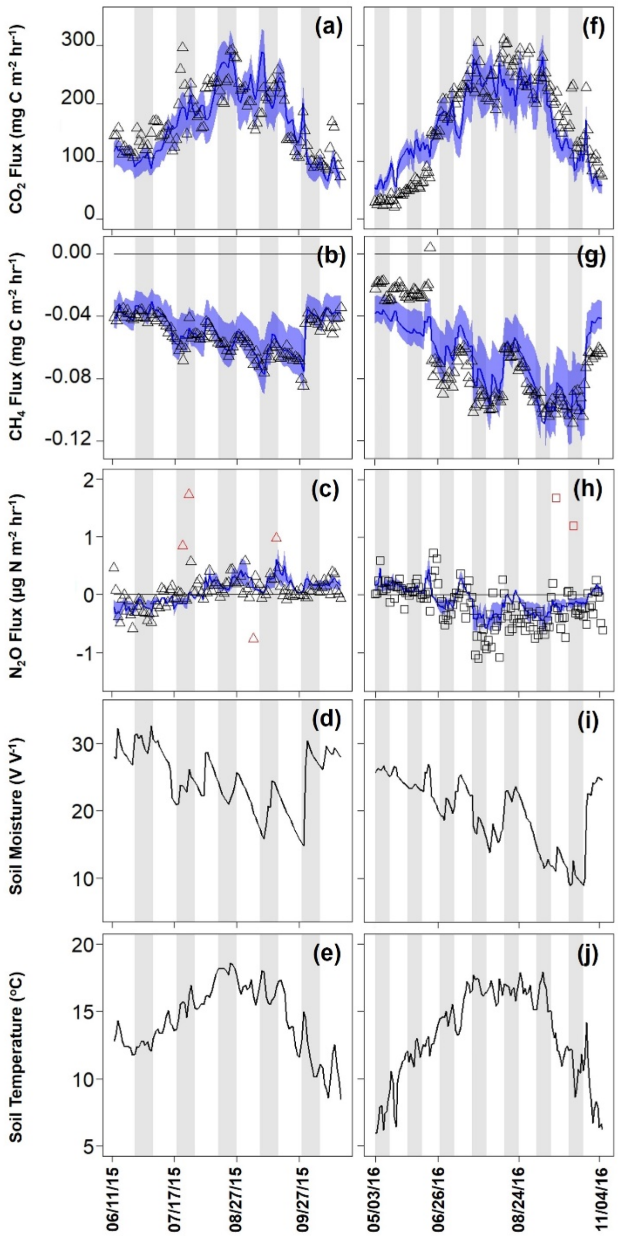

Fig. 2: Temporal trend of greenhouse (GHG) gas (CO_2: a, f; CH_4: b, g; and N_2O: c, h) fluxes, soil moisture (d, i), and soil temperature (e, j) during 2015 (a-e) and 2016 (f-j) growing seasons. Triangles and squares represent observed GHG fluxes in 2015 and 2016, respectively. Light gray shades in the background represent validation windows, which are interspersed throughout the observation period. Red triangles and squares represent outliers for N_2O fluxes. Blue line and shade represent median and 95% CI of simulated GHG fluxes.

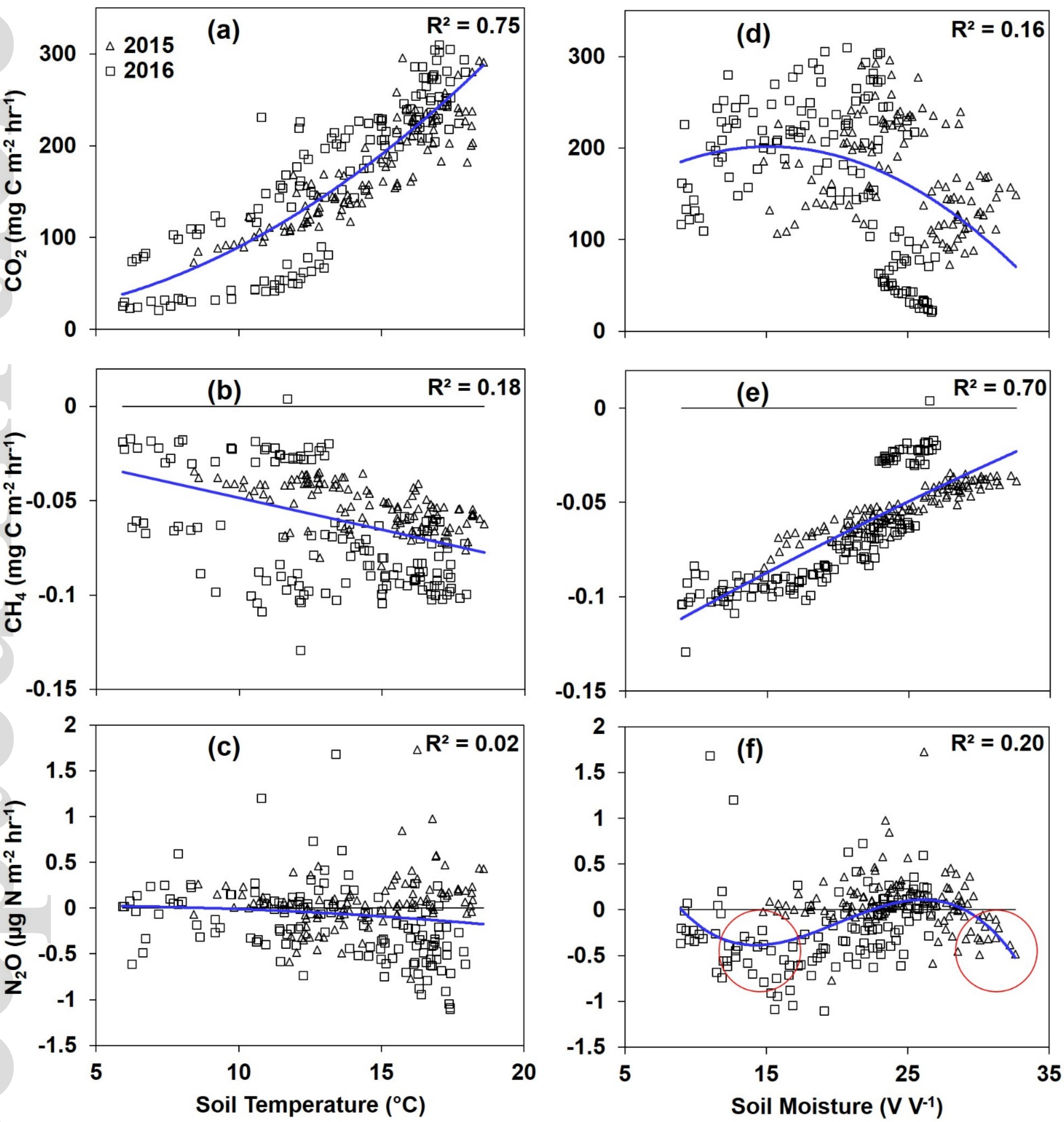

Fig. 3: Relation of observed CO_2 (a, d), CH_4 (b, e), and N_2O (c, f) fluxes with soil temperature (a-c) and soil moisture (b-e). Triangles and squares represent observed GHG fluxes in 2015 and 2016, respectively.

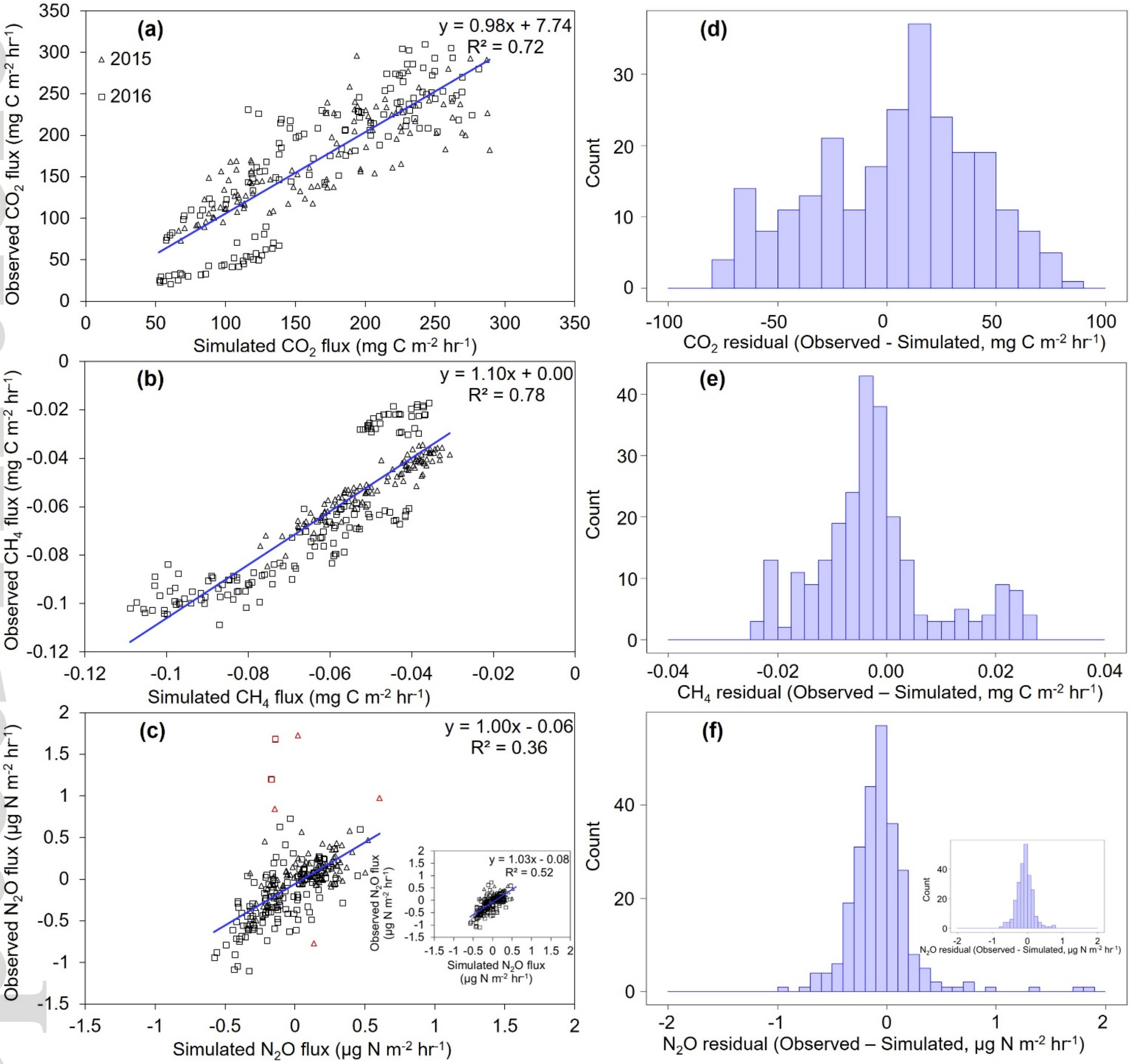

Fig. 4: Relation between observed versus simulated greenhouse gas, GHG (CO_2 (a, d), CH_4 (b, e), and N_2O (c, f)) fluxes. Triangles and squares in a-c represent observed GHG fluxes in 2015 and 2016, respectively. Red triangles and squares in lower left panel (c) represent outliers for N_2O fluxes. Inset figures in bottom panels (c, f) represent one-to-one relation and model residuals for N_2O after removing the outliers.

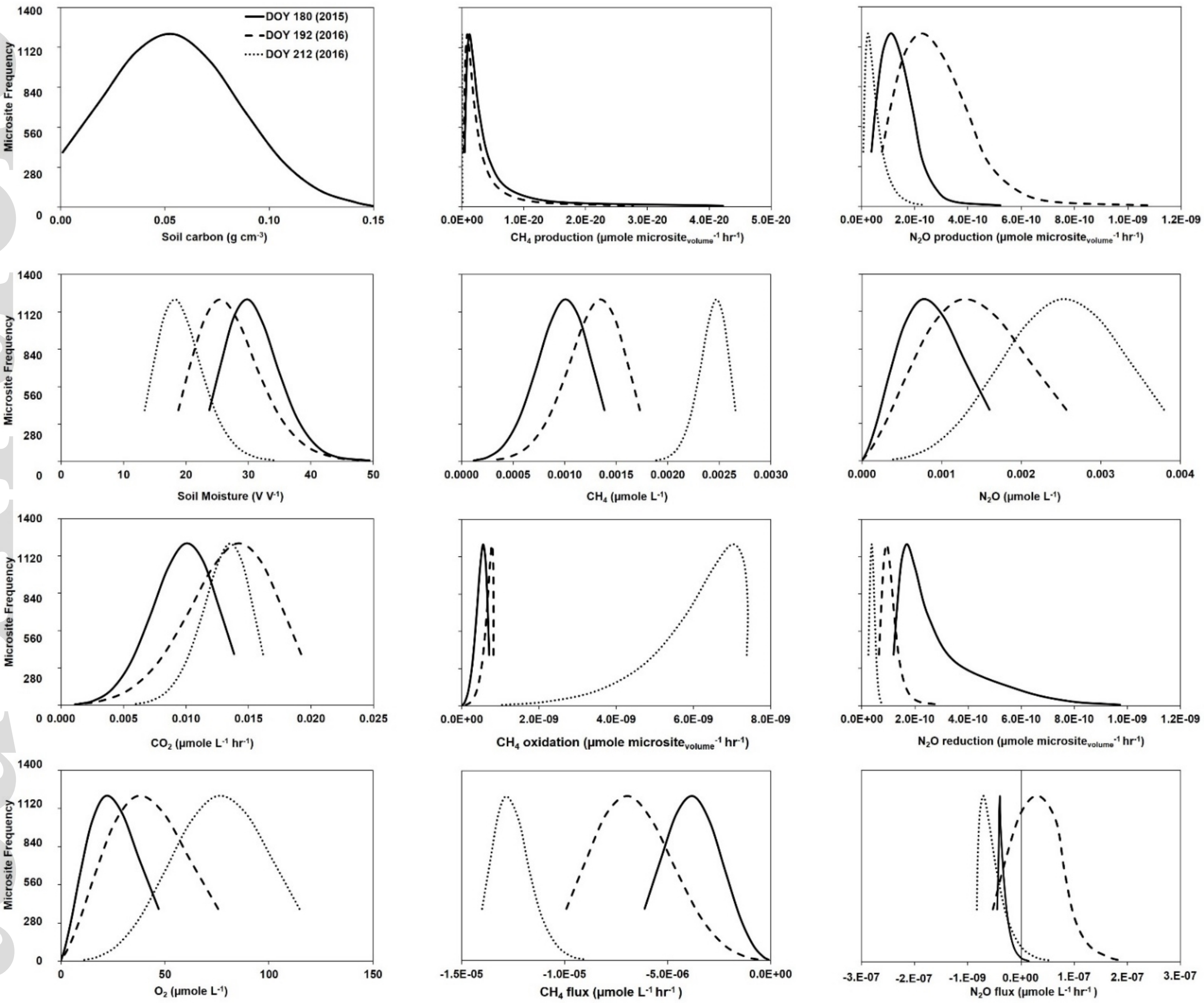

Fig. 5: Microsite probability distribution functions (PDFs) of soil carbon (a), soil moisture (b), CO_2 flux (c), O_2 concentration (d), CH_4 production (e), CH_4 concentration (f), CH_4 oxidation (g), CH_4 flux (h), N_2O production (i), N_2O concentration (j), N_2O reduction (k), and N_2O flux (l). Solid, dashed, and dotted lines represent simulated microsite PDFs of individual processes for DOY 180, 2015 (SoilM=32.6 v v^{-1} & SoilT=12.0 °C); DOY 192, 2016 (SoilM=25.4 v v^{-1} & SoilT=13.8 °C); and DOY 212, 2016(SoilM=18.2 v v^{-1} & SoilT=16.3 °C), respectively, and correspond to three scenarios presented in the discussion section. DOY: Day of year, SoilM: Soil moisture, SoilT: Soil temperature.

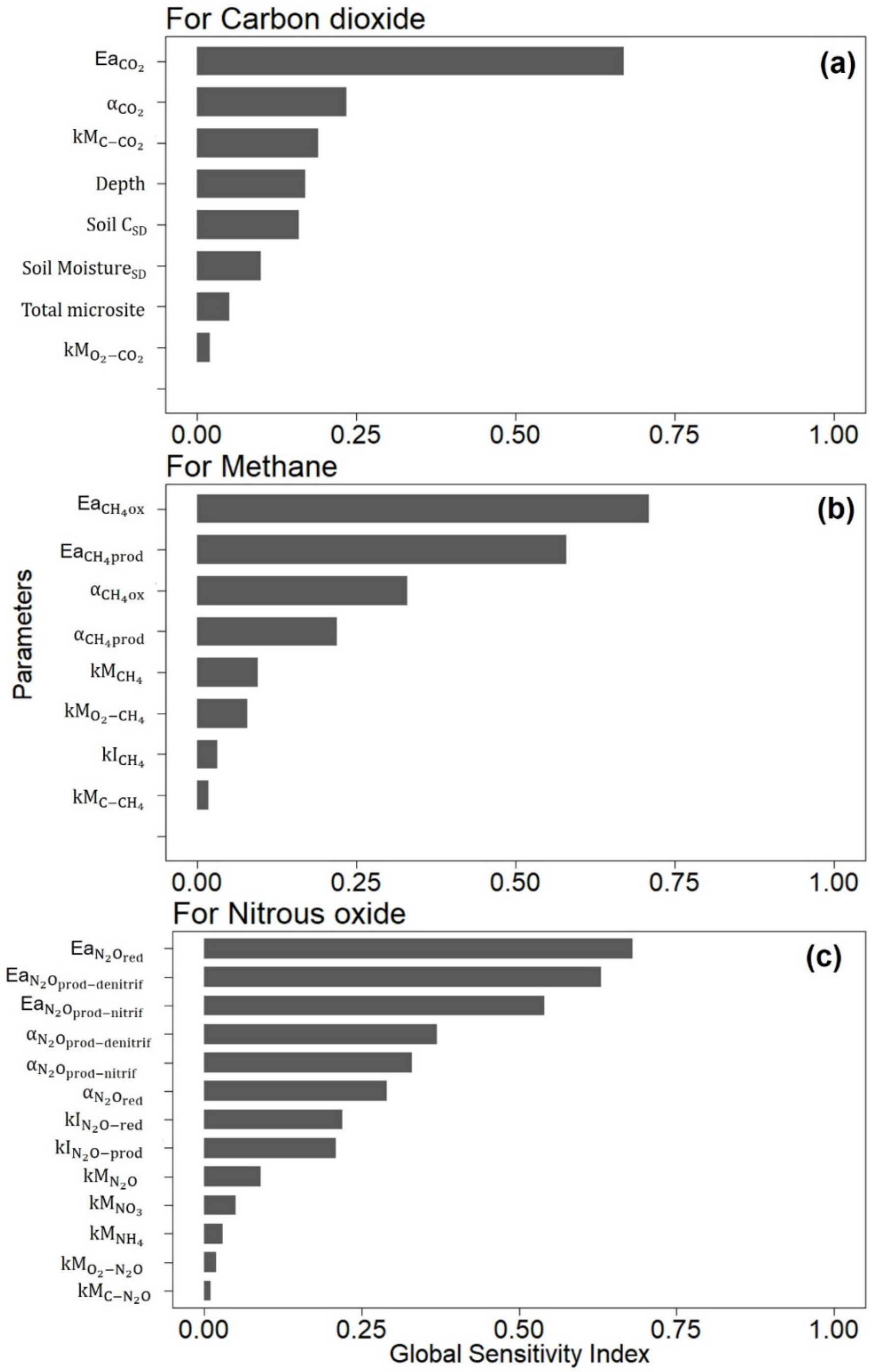

Fig. 6: Sensitivity indices of the DAMM-GHG model parameters for CO_2 (a), CH_4 (b), and N_2O (c) modules, respectively.

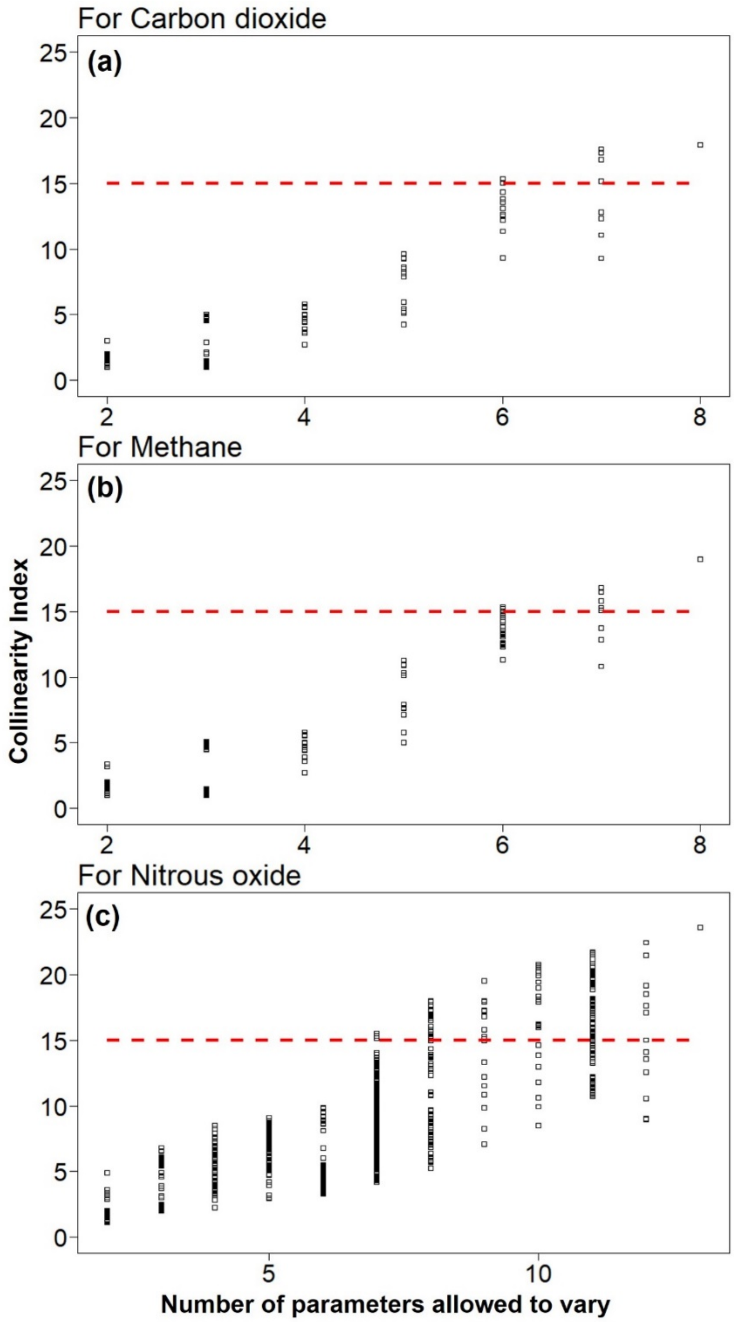

Fig. 7: Collinearity indices of the DAMM-GHG model parameters for CO_2 (a), CH_4 (b), and N_2O (c) modules, respectively. Each point represents a unique combination of parameters allowed to vary while others are held constant. Dashed horizontal lines represent threshold value above which approximate linear dependence of model parameters increases and poor identifiability can be expected (Omlin et al., 2001).

Discussion

Our goal is a novel integration of measurement and modeling of three key greenhouse gases to improve understanding of and modeling capacity for interactions of belowground temperature, moisture, and substrate supply that control the net soil emissions of CO_2, CH_4, and N_2O. To this end, we built upon the DAMM model, which mechanistically simulates soil heterotrophic respiration using Arrhenius equations, diffusion functions, and Michaelis-Menten enzyme kinetics (Davidson et al., 2012, 2014). Our framework of the DAMM-GHG model is unique in that it represents the simultaneous production and consumption of all three GHGs within the same soil biophysical framework using microsite PDFs. Below we discuss the performance of the DAMM-GHG model and the utility of the microsite PDFs in reproducing the spatial and temporal dynamics of observed CO_2, CH_4, and N_2O fluxes within a multiple constraint framework.

Microsite Representation Captures Co-occurrence of Methane Oxidation and Nitrous Oxide Reduction

Consumption of atmospheric N_2O via classical denitrification should occur only under reducing conditions. Yet, we have observed net uptake of atmospheric CH_4 (oxidation) and uptake of atmospheric N_2O (reduction) simultaneously in well-drained soils of Howland forest under both low and high soil moisture levels. With the advent of high frequency and high sensitivity flux measurement technology, we can be confident that these modest uptake rates of both CH_4 and N_2O are significantly different from zero and are not measurement errors or artifacts (Fig. 2 and 4, also see Fig. S4). These seemingly contradictory observations have been qualitatively explained by describing diffusional constraints of gas transport as follows: both CH_4 and N_2O can diffuse into well-drained soils; the CH_4 is oxidized at microsites where O_2 is abundant; while N_2O is reduced at other microsites where N_2O is present and heterotrophic respiration is sufficiently rapid to consume O_2. Here, we demonstrate that this qualitative explanation can be expressed in a mathematically consistent biophysical process model that is numerically consistent with simultaneously measured fluxes of these gases.

The area under a soil chamber was partitioned according to a bivariate lognormal PDF of soil C and moisture across a range of microsites, which leads to a PDF of CO_2 production and O_2 consumption among microsites. The resulting broad range of microsite O_2 concentrations determines the PDF of microsites that produce or consume CH_4 and N_2O according to Michaelis-Menten and Arrhenius functions for each process (Figs. 1, S1). Concentrations of below ambient N_2O (hotspots of N_2O reduction) occur in microsites with simulated high C and high moisture. Net consumption and production of CH_4 and N_2O are simulated within a chamber as the average of all soil microsite simulations. To demonstrate that it is numerically feasible for microsites of N_2O reduction and CH_4 oxidation to co-occur under a single chamber, we discuss three different scenarios where mean soil moisture levels cover the envelope of observed soil moisture in our study area (Fig. 5).

Of the two growing seasons, we measured highest bulk soil moisture (32.6 V V^{-1}) on June 29 (DOY 180), 2015. Consequently, microsite PDFs of soil moisture ranged between 23.7 V V^{-1} to as high as 47.7 V V^{-1} (solid line in Fig. 5b). Microsites with high soil moisture limited diffusion of gaseous O_2 through air-filled pore space. Simultaneously, soils had warmed up enough during the late spring of 2015 for soil respiration to exceed 100 mg CO_2-C m^{-2} hr^{-1}, which created significant O_2 demand in microsites with high soil C. Relatively high soil respiration along with limited O_2 diffusion resulted in a large fraction of total soil microsites with low O_2 concentrations (solid line in Fig. 5d). Production of N_2O was high in microsites with high soil C. However, reducing environments favored N_2O reduction more than N_2O production in microsites with low O_2 concentrations. Together, the PDFs of soil microsites resulted in a modest net negative mean flux of N_2O (solid line in Fig. 5l). Classical theories of biological denitrification processes fit with our observations of net negative fluxes of N_2O under conditions of high soil moisture (and soil C) when enzymatic reduction of N_2O to N_2 under reducing environment outcompete N_2O production rates, especially in nitrogen-limited systems like our field site (Davidson et al., 1993, 2000; Firestone & Davidson, 1989). Although N_2O reduction slightly exceeded N_2O production under these conditions, net uptake rates of atmospheric N_2O were low, because diffusion of atmospheric N_2O into the soil, while occurring and thus supporting some uptake, was also limited by high water-filled pore space.

The diffusion of atmospheric N_2O into the soil increased during the drier 2016 summer, thus enabling somewhat larger net uptake of atmospheric N_2O. The observed soil moisture content of 18.2 V V^{-1} on July 30 (DOY 212), 2016 approximately represents the 1st quantile of observed soil moisture across 2015 and 2016 growing seasons. Rates of N_2O production during nitrification and denitrification were low in a large majority of microsites due to the oxygen inhibition effects as well as the diffusional constraints of soil C, ammonium, and nitrate substrates at low soil moisture. However, greater diffusion of atmospheric N_2O to soil microsites also increased the microsite concentrations of N_2O (dotted line in Fig. 5j), including a small fraction of microsites with sufficiently low O_2 concentrations to not fully inhibit N_2O reduction (i.e., the simulated O_2 was near the kI for N_2O reduction (kI_{N_2O-red}) in approximately 10% of total microsites, resulting in net negative flux of N_2O (dotted line in Fig. 5d, Table 1). Our observation of a net soil sink of atmospheric N_2O during summer drying events match with reports from other natural and managed ecosystems, ranging from tropical to temperate climates, where net uptake of atmospheric N_2O has been measured when mean bulk soil moisture was drier than would normally be expected for N_2O reduction (Donoso et al., 1993; Flechard et al., 2005; Goldberg & Gebauer, 2009; Verchot et al., 2000; Yamulki et al., 1995). In this case, however, we can demonstrate quantitatively that reducing conditions in only about 10% of the microsites was sufficient to enable net uptake of atmospheric N_2O.

In contrast to the above two examples, intermediate soil moisture conditions are favorable for production to exceed consumption, resulting in modest net emissions of N_2O from soil to the atmosphere. Within this context, observed soil moisture content of 25.4 V V^{-1} on July 10, 2016 (DOY 192; dashed lines in Fig. 5), approximately represents the 3rd quantile of observed soil moisture across 2015 and 2016 growing seasons (Fig. 5b). As expected, N_2O production was greatest at this intermediate soil moisture (Fig. 5j), especially in microsites with high soil C. Because N_2O production was much higher than the very low N_2O reduction rates (Fig. 5k) in a sufficiently large number of total soil microsites, a net positive mean N_2O flux resulted (Fig. 5l).

Previous studies indicated that N_2O production during biological nitrification and denitrification often peak at 50-80% of water-filled pore-space (Davidson, 1991; Metivier et al., 2009), when soil moisture may be sufficiently high such that nitrate and nitrite are more available than O_2 as the alternate elector acceptor in many microsites, but the soil O_2 content is still high enough to mostly inhibit the reduction of N_2O to N_2. This is the basis of the soil moisture function of the conceptual hole-in-the-pipe model (Firestone and Davidson, 1989). This relationship between soil moisture and N_2O production is often represented in models as an empirical statistical algorithm, such as a polynomial or similar function (e.g., Del Grosso et al., 2001; Potter et al., 1996). In contrast, the responses to soil moisture in the DAMM-GHG model produces the response pattern across simulated microsites (Fig. S7) predicted by the conceptual hole-in-the-pipe model as an emergent property of the role of O_2 as substrate (for nitrification, see Fig. S1) or inhibitor, as represented by different kI values ($kI_{N_2O-prod}$ and kI_{N_2O-red}) used in DAMM mechanistic functions (Table 1).

For CH_4, the microsite PDFs of production, consumption, and net emission were relatively straightforward. Methane production was high in a relatively few numbers of microsites with high soil moisture (and soil C). In contrast, CH_4 oxidation was high in the majority of microsites, which had low soil moisture, as the diffusion of both substrates (O_2 and CH_4) increased with decreasing soil moisture. Note that CH_4 production was several orders of magnitude lower than CH_4 oxidation across the simulated range of microsite moisture contents in our study, mainly due to significant oxygen inhibition. Therefore, microsite PDFs of CH_4 oxidation primarily dominated the net CH_4 emission, where net CH_4 emission linearly decreased with decreasing soil moisture (Fig. 5e-h).

Taken together, these results demonstrate that representing production, consumption, and diffusion processes as a function of soil microsite PDFs can neatly encapsulate the factors affecting emissions of CO_2, CH_4, and N_2O in field studies and their underlying mechanisms. We also did a comparison of the model performance to a conventional framework, where we kept identical soil C and soil moisture values, set to the average values observed for the bulk soil, across all microsites. Although the performance of the model without microsite PDF was comparable to the one with microsite PDF for CO_2, model performance for CH_4 and N_2O was strongly affected by microsite variability (Figs. S8, S9). The model without microsite PDF simulated less uptake of CH_4 overall, had larger than observed peaks and valleys during in wet-up and dry-down events, and had more biased residuals (Figs. S8b, S8g, S9b, S9e). For N_2O, the model with PDF representation of microsite variation also had an overall better fit to the observations and less biased residuals (Figs. S8c, S8h, S9c, S9f).

The model-data fusion algorithm we used tends to reduce the overall model-data mismatch for the entire measurement window, and so it is not surprising that there are periods within that window where simulations do not match observations as well, such as the CO_2 and CH_4 fluxes of spring 2016 (Fig. 2). This may also be due to other factors not included in the DAMM-GHG model, such as impacts of spring freeze-thaw cycles on C availability or phenology of root exudates. Additionally, the lower fraction of observed variability of N_2O fluxes accounted for by the model, compared to CO_2 and CH_4 fluxes, can be attributed to; (1) the low signal-to-noise ratio inherent to very low N_2O fluxes; and (2) the increased number and complexity of interactions of substrates (and inhibitors) for production (e.g. C, O_2, NH_4^+, and NO_3^-) and consumption (e.g. C, O_2, and N_2O) of N_2O during nitrification and denitrification that are represented numerically in the model with additional parameters (Figs. 2, 4). We further discussed how these potential interacting processes might have increased the covariation of parameters related to N_2O dynamics than those related to CO_2 and CH_4 dynamics (see *Collinearity analysis* subheading).

Sensitivity Analysis

Sensitivity of Predicted Greenhouse Gas Fluxes to Model Parameters

Sensitivity indices indicated that the parameters representing the Vmax terms in the Arrhenius equation (α and Ea) for production and consumption of each gas were the most influential for all three GHGs (Fig. 6a-c), which is in line with other reports (Abramoff et al., 2017; Zarnetske et al., 2012). Sensitivity of GHG fluxes to the parameters representing Michaelis-Menten equations were secondary to those of the α(s) and Ea(s), where the individual ranking was associated with the importance of controlling drivers. Following α(s) and Ea(s), some of the half-saturation constants, i.e. kM(s), were more important than others. For example, relatively higher sensitivity indices of the half-saturation constants of CH_4 (kM_{CH_4}) and O_2 ($kM_{O_2-CH_4}$) for CH_4 oxidation as compared to the half-saturation constants of C (kM_{C-CH_4}) and inhibition coefficient of O_2 (kI_{CH_4}) for CH_4 production can be explained by the dominant role of CH_4 oxidation in controlling net CH_4 emissions in our study. On the other hand, the inhibition coefficients of O_2 for N_2O reduction (kI_{N_2O-red}) and N_2O production ($kI_{N_2O-prod}$), along with the half-saturation constant of N_2O for N_2O reduction (kM_{N_2O}), had relatively higher sensitivity indices than those for the half-saturation constant of ammonium (kM_{NH_4}) and O_2 ($kM_{O_2-N_2O}$) during nitrification and nitrate (kM_{NO_3}) and C (kM_{C-N_2O}) during denitrification, respectively. These results indicate the greater importance of reducing conditions and the diffusive supply of N_2O in controlling net N_2O emission at our site than either the concentrations of NH_4^+ and O_2 substrates for nitrification or NO_3^- and C substrates for denitrification. This result may be particular to our site where NO_3^- is uniformly low and the seasonal trend of NH_4^+ is much less dynamic than that of soil moisture (Fernandez et al., 1995). We speculate that kM_{NH_4} and kM_{NO_3}

might be more commonly important in agricultural soils, where large temporal variations in NH_4^+ and NO_3^- are expected depending upon the timing of fertilization and crop uptake.

Sensitivity of Predicted Greenhouse Gas Fluxes to Model Drivers

Soil moisture primarily (and soil temperature secondarily) controlled the skewness of the microsite PDFs of production, consumption, and diffusion processes of each gas (Fig. S10). Within this context, it is important to note that even though the parameters representing the Vmax terms in the Arrhenius equation (Ea and α) had higher sensitivity indices than the Michaelis-Menten parameters that represent the influence of soil moisture (Fig. 6a-c), most of the temporal variations in CH_4 and N_2O fluxes were nevertheless explained by soil moisture rather than temperature. The correlation matrix in Fig. S5 also indicates that soil moisture, rather than soil temperature, controlled the temporal variation of CH_4 and N_2O fluxes. In other words, if the Ea value is changed, the average simulated flux for the entire time period increases or decreases significantly, but the within-season variation in CH_4 and N_2O fluxes is still dominantly influenced by variation in soil moisture (Figs. S6, S10).

Collinearity analysis

As expected, the collinearity index (CI) increases as the number of variable parameters increases (Fig. 7). Given the parsimonious model structure, we had few problems of identifiability of the processes for CO_2 and CH_4 module, and the most parameter combinations remain below the threshold value of 15 (Brun et al., 2002; Omlin et al., 2001). However, we do have some parameter combinations with CI>15 for the N_2O module, due to probable ambiguity of whether N_2O fluxes are affected more by production via nitrification (affected by NH_4^+ substrate), production via denitrification (affected by NO_3^- substrates), or consumption of N_2O (affected by N_2O diffusion). Tradeoffs of processes within models can account for inflation of CI values (Keenan et al., 2011; Richardson et al., 2010), which is likely the case for the N_2O module relative to the CO_2 and CH_4 modules. Overall, however, collinearity analysis indicates that the chances of having equifinality issues characterized by biologically improbable process representations were generally low in the DAMM-GHG model.

We believe that this success is largely due to the multiple constraints imposed by simultaneously modeling data streams of three different gases, which enabled us to capture the influence of temporally and spatially varying drivers on GHG fluxes (Myrgiotis et al., 2018). For example, when simulating only CH_4 flux, a better fit of the model to the data might be achieved by adjusting either the Michaelis-Menten parameters or the diffusion parameters, but it may be impossible to know which the "correct" adjustment is. However, if N_2O and CO_2 are also being simultaneously simulated, then adjusting the diffusion parameters will affect simulations of all three gases, whereas adjusting the Michaelis-Menten parameters for CH_4 oxidation should have little effect on the other two gases. Hence, the additional constraints help identify which model parameterizations are consistent with all three data streams of flux measurements.

Microsite probability distribution functions permit model parsimony

Simulating a 3-D array of soil aggregates or pore-networks (Arah & Vinten, 1995; Ebrahimi & Or, 2014; Yan et al., 2016) is another approach for representing spatial heterogeneity of soil matrix in biogeochemical models. However, explicit representation of soil spatial variability requires detailed information on soil structure, involving high-throughput instrumentations such as X-ray CT scan (see Carducci et al., 2017) and may require greater computational power than our PDF approach. Because of the limited measurements on the spatial variability of soil aggregates (or pores) at a plot scale, let alone at larger scales, and because of the increased computational complexity in spatially explicit model structures, scaling up of 3-D soil aggregate (or pore-network) models to the ecosystem models and ESMs is still challenging.

Statistically representing microsite variation as PDFs in the DAMM-GHG model offers a relatively computationally efficient, yet mechanistically consistent, alternative way of simulating soil heterogeneity and maintaining model parsimony, as in the original DAMM model (Davidson et al., 2012, 2014; Sihi et al., 2018). We believe that our framework could be used to simulate fluxes of GHGs from other natural and managed systems as well as be scaled up to ecosystem models and ESMs.

Opportunities for Future Improvement of the DAMM-GHG Model

We represented all microsite-scale processes by optimizing an equivalent depth for heterotrophic respiration, where most of the biological reactions appear to happen in the soil of this study site (posterior range: 6-11 cm) and fixed that depth for simulating processes related to production and consumption of CH_4 and N_2O. This simplification allowed us to use unitless diffusion constants for gaseous and dissolved substrates and to avoid needing to know exact diffusion path lengths (see Davidson et al., 2012 for details). Exploring heterogeneity of diffusivity within and among soil horizons could be an appropriate next step.

Including more complex models of gas diffusion that includes variable diffusivity between intra-aggregate and inter-aggregate pore spaces may be more appropriate for aggregated media like soil (Millington and Shearer, 1971; Resurreccion et al., 2010). Representing soil microsite PDFs in more than one vertically stratified soil horizon by differentiating between the organic and various mineral horizons may be needed for application to other sites (e.g. wetland with a seasonally variable depth to the water table), such that transport of gases between soil horizons and across soil-air boundary can be estimated using Fick's law. Measured vertical concentration profiles of soil gases could serve as additional data constraints for soil gas concentration profiles that become emergent simulated properties of this modeling approach. It would also be useful to have a data stream of heterogeneity of O_2 or redox potentials across microsites, but that would require new generations of micro-probes.

Additionally, techniques that disentangle gross production and gross consumption rates of CH_4 and N_2O under field conditions could increase the predictive power of the dynamics of soil GHGs fluxes. For example, Chanton et al. (2007) reported that measuring stable carbon isotope of emitted CH_4 ($^{13}CH_4$) is a feasible way to quantify gross CH_4 oxidation in-situ. Likewise, Wen et al. (2018) demonstrated that $^{15}N_2O$ pool dilution method can be effective to measure atmospheric N_2O uptake in soil under field conditions. In-situ quantification of microbial activities pertaining to gross production and consumption of CH_4 and N_2O can also be pursued following the gas push-pull method (Urmann et al., 2005). Quantifying gross nitrogen transformations using stable isotope tracing could help constrain the sources of N_2O emissions (Morse & Bernhardt, 2013; Müller et al., 2007; Myrold et al., 1986).

In addition to nitrification and biological denitrification, other bacterial (Jensen & Burris, 1986; Yamazaki et al., 1987) and fungal (Hayatsu et al., 2008; Shoun et al., 1992) contributions, as well as abiotic (Davidson et al., 2003; Vieten 2008) sinks of N_2O in soil could be explored if warranted. Adding other controlling factors, such as pH effects, temporal dynamics of enzyme synthesis, root exudation, could improve model performance for some sites (Butterbach-Bahl et al., 2013; Zheng & Doskey, 2015). In all of these cases, however, the potential additional explanatory value of more parameters and model complexity must be balanced with the availability of data to constrain them and with the advantages of model structure parsimony.

Conclusions

Representing microsite heterogeneity as PDFs related to predictive processes offers a new approach for numerical representation of methanogenesis, methane oxidation, nitrification, and denitrification and other spatially and temporally variable microbial processes in soil. Our ability to accurately measure and skillfully model rates of these processes has been hampered by highly variable soil microsite conditions, which are difficult to measure and simulate, but our use of PDFs to represent that variability offers a promising and computationally efficient approach. In addition, by measuring and modeling all three greenhouse gases (CO_2, CH_4, and N_2O), we have mechanistically and quantitatively explained the apparent paradox of observed simultaneous aerobic respiration that produces CO_2, CH_4 uptake (oxidation), CH_4 production, and N_2O uptake (reduction) in the same soil profile. Skillful representations of multiple ecologically relevant processes increase confidence of getting the right answers for the right reasons. This relatively parsimonious process modeling framework has the potential to be implemented within ecosystem models and ESMs to better capture the dynamics of soil-based greenhouse gases at landscape, regional, and global scales.

Acknowledgments

This work was supported by the USDA NIFA award # 2014-67003-22073. Research activities at the Howland Forest is supported by the USDA Forest Service's Northern Research Station and the US Department of Energy's BER (Office of Science) program. We thank Dr. Andrew D. Richardson for facilitating our access to the Odyssey cluster supported by the FAS Division of Science at the Harvard University, which we used for computational purposes. All data used in this paper are available through Richardson et al (2019). R scripts used for this modeling work are made available as a GitHub repository (https://github.com/dsihi/DAMM-GHG).

References

Abramoff, R. Z., Davidson, E. A., & Finzi, A. C. (2017). A parsimonious modular approach to building a mechanistic belowground carbon and nitrogen model. *Journal of Geophysical Research: Biogeosciences, 122*(9), 2418-2434. doi:doi:10.1002/2017JG003796

Abramoff, R. Z., Xu, X., Hartman, M., O'Brien, S., Feng, W., Davidson, E., A. . . . Mayes, M. A. (2018). The Millennial model: in search of measurable pools and transformations for modeling soil carbon in the new century. Biogeochemistry, 137(1), 51-71. doi:10.1007/s10533-017-0409-7

Angert, A., Yakir, D., Rodeghiero, M., Preisler, Y., Davidson, E. A., & Weiner, T. (2015). Using O_2 to study the relationships between soil CO_2 efflux and soil respiration. Biogeosciences, 12, 2089-2099.

Arah, J. R. M. and K. D. Stephen (1998). "A model of the processes leading to methane emission from peatland." Atmospheric Environment 32(19): 3257-3264.

Arah, J. R. M., & Vinten, A. J. A. (1995). Simplified models of anoxia and denitrification in aggregated and simple-structured soils. European Journal of Soil Science, 46(4), 507-517. doi:doi:10.1111/j.1365-2389.1995.tb01347.x

Arrhenius, S. (1889). Über die Reaktionsgeschwindigkeit bei der Inversion von Rohrzucker durch Säuren. In *Zeitschrift für Physikalische Chemie* (Vol. 4U, pp. 226).

Bernhardt, E. S., Blaszczak, J. R., Ficken, C. D., Fork, M. L., Kaiser, K. E., & Seybold, E. C. (2017). Control points in ecosystems: Moving beyond the hot spot hot moment concept. *Ecosystems, 20*(4), 665-682.

Bidot C, Lamboni M, Monod H (2018). _multisensi: Multivariate Sensitivity Analysis_. R package version 2.1-1, <URL: https://CRAN.R-project.org/package=multisensi>.

Bodelier, P., Libochant, J. A., Blom, C., & Laanbroek, H. J. (1996). Dynamics of nitrification and denitrification in root-oxygenated sediments and adaptation of ammonia-oxidizing bacteria to low-oxygen or anoxic habitats. Appl. Environ. Microbiol., 62(11), 4100-4107.

Brewer, P., Calderón, F., Vigil, M., & von Fischer, J. (2018). Impacts of moisture, soil respiration, and agricultural practices on methanogenesis in upland soils as measured with stable isotope pool dilution. *Soil Biology and Biochemistry, 127*, 239-251.

Brun, R., Kühni, M., Siegrist, H., Gujer, W., & Reichert, P. (2002). Practical identifiability of ASM2d parameters—systematic selection and tuning of parameter subsets. Water Research, 36(16), 4113-4127. doi:https://doi.org/10.1016/S0043-1354(02)00104-5

Brun, R., Reichert, P., & Künsch, H. R. (2001). Practical identifiability analysis of large environmental simulation models. Water Resources Research, 37(4), 1015-1030. doi:doi:10.1029/2000WR900350

Butterbach-Bahl, K., Baggs, E. M., Dannenmann, M., Kiese, R., & Zechmeister-Boltenstern, S. (2013). Nitrous oxide emissions from soils: how well do we understand the processes and their controls? *Philosophical Transactions of the Royal Society B: Biological Sciences, 368*(1621), 20130122. doi:doi:10.1098/rstb.2013.0122

Canion, A., Kostka, J. E., Gihring, T. M., Huettel, M., van Beusekom, J. E. E., Gao, H., . . . Kuypers, M. M. M. (2014). Temperature response of denitrification and anammox reveals the adaptation of microbial communities to in situ temperatures in permeable marine sediments that span 50° in latitude. Biogeosciences, 11(2), 309-320. doi:10.5194/bg-11-309-2014

Carbone, M. S., Richardson, A. D., Chen, M., Davidson, E. A., Hughes, H., Savage, K. E., & Hollinger, D. Y. (2016). Constrained partitioning of autotrophic and heterotrophic respiration reduces model uncertainties of forest ecosystem carbon fluxes but not stocks. Journal of Geophysical Research: Biogeosciences, 121(9), 2476-2492. doi:doi:10.1002/2016JG003386

Carducci, C. E., Zinn, Y. L., Rossoni, D. F., Heck, R. J., & Oliveira, G. C. (2017). Visual analysis and X-ray computed tomography for assessing the spatial variability of soil structure in a cultivated Oxisol. Soil and Tillage Research, 173, 15-23. doi:https://doi.org/10.1016/j.still.2016.03.006

Cattânio, J. H., Davidson, E. A., Nepstad, D. C., Verchot, L. V., & Ackerman, I. L. (2002). Unexpected results of a pilot throughfall exclusion experiment on soil emissions of CO2, CH4, N2O, and NO in eastern Amazonia. *Biology and Fertility of Soils, 36*(2), 102-108. doi:10.1007/s00374-002-0517-x

Chanton, J. P., Powelson, D. K., Abichou, T., & Hater, G. (2008). Improved Field Methods to Quantify Methane Oxidation in Landfill Cover Materials Using Stable Carbon Isotopes. Environmental Science & Technology, 42(3), 665-670. doi:10.1021/es0710757

Chapuis-Lardy, L., Wrage, N., Metay, A., CHOTTE, J. L., & Bernoux, M. (2007). Soils, a sink for N2O? A review. *Global Change Biology, 13*(1), 1-17.

Ciais, P., Sabine, C., Bala, G., Bopp, L., Brovkin, V., Canadell, J., . . . Heimann, M. (2014). Carbon and other biogeochemical cycles. In Climate change 2013: the physical science basis. Contribution of Working Group I to the Fifth Assessment Report of the Intergovernmental Panel on Climate Change (pp. 465-570): Cambridge University Press.

Conrad, R. (1996). Soil microorganisms as controllers of atmospheric trace gases (H2, CO, CH4, OCS, N2O, and NO). *Microbiological reviews, 60*(4), 609-640.

Conrad, R. (2009). The global methane cycle: recent advances in understanding the microbial processes involved. *Environmental Microbiology Reports, 1*(5), 285-292. doi:doi:10.1111/j.1758-2229.2009.00038.x

Crill, P., Martikainen, P., Nykanen, H., & Silvola, J. (1994). Temperature and N fertilization effects on methane oxidation in a drained peatland soil. Soil Biology and Biochemistry, 26(10), 1331-1339.

Davidson, E. A. (1991). Fluxes of nitrous oxide and nitric oxide from terrestrial ecosystems. *Microbial Production and Consumption of Greenhouse Gases: Methane, Nitrous Oxide, and Halomethanes*, 219-235.

Davidson, E. A., Belk, E., & Boone, R. D. (1998). Soil water content and temperature as independent or confounded factors controlling soil respiration in a temperate mixed hardwood forest. *Global Change Biology, 4*(2), 217-227. doi:doi:10.1046/j.1365-2486.1998.00128.x

Davidson, E. A., Chorover, J., & Dail, D. B. (2003). A mechanism of abiotic immobilization of nitrate in forest ecosystems: the ferrous wheel hypothesis. Global Change Biology, 9(2), 228-236. doi:doi:10.1046/j.1365-2486.2003.00592.x

Davidson, E. A., & Janssens, I. A. (2006). Temperature sensitivity of soil carbon decomposition and feedbacks to climate change. *Nature, 440*, 165. doi:10.1038/nature04514

Davidson, E. A., Janssens, I. A., & Luo, Y. (2006). On the variability of respiration in terrestrial ecosystems: moving beyond Q10. *Global Change Biology, 12*(2), 154-164. doi:doi:10.1111/j.1365-2486.2005.01065.x

Davidson, E. A., Keller, M., Erickson, H. E., & Verchot, L. V., Veldkamp, E. (2000). Testing a Conceptual Model of Soil Emissions of Nitrous and Nitric Oxides: Using two functions based on soil nitrogen availability and soil water content, the hole-in-the-pipe model characterizes a large fraction of the observed variation of nitric oxide and nitrous oxide emissions from soils. BioScience, 50(8), 667-680. doi:10.1641/0006-3568(2000)050[0667:Tacmos]2.0.Co;2

Davidson, E. A., Matson, P. A., Vitousek, P. M., Riley, R., Dunkin, K., Garcia-Mendez, G., & Maass, J. M. (1993). Processes Regulating Soil Emissions of NO and N_2O in a Seasonally Dry Tropical Forest. Ecology, 74(1), 130-139. doi:doi:10.2307/1939508

Davidson, E. A., Samanta, S., Caramori, S. S., & Savage, K. (2012). The Dual Arrhenius and Michaelis–Menten kinetics model for decomposition of soil organic matter at hourly to seasonal time scales. *Global Change Biology, 18*(1), 371-384. doi:doi:10.1111/j.1365-2486.2011.02546.x

Davidson, E. A., Savage, K. E., & Finzi, A. C. (2014). A big-microsite framework for soil carbon modeling. *Global Change Biology, 20*(12), 3610-3620. doi:doi:10.1111/gcb.12718

Dean, J. F., Middelburg, J. J., Röckmann, T., Aerts, R., Blauw, L. G., Egger, M., . . . Dolman, A. J. (2018). Methane Feedbacks to the Global Climate System in a Warmer World. *Reviews of Geophysics, 56*(1), 207-250. doi:doi:10.1002/2017RG000559

Del Grosso, S., Parton, W., Mosier, A., Hartman, M., Keough, C., Peterson, G., . . . Schimel, D. (2001). Simulated effects of land use, soil texture, and precipitation on N gas emissions using DAYCENT. In Nitrogen in the Environment: Sources, Problems and Management (pp. 413-431): Elsevier.

Donoso, L., Santana, R., & Sanhueza, E. (1993). Seasonal variation of N2O fluxes at a tropical savannah site: Soil consumption of N2O during the dry season. Geophysical Research Letters, 20(13), 1379-1382. doi:doi:10.1029/93GL01537

Ebrahimi, A., & Or, D. (2018). On Upscaling of Soil Microbial Processes and Biogeochemical Fluxes From Aggregates to Landscapes. Journal of Geophysical Research: Biogeosciences, 123(5), 1526-1547. doi:doi:10.1029/2017JG004347

Eugster, W., Zeyer, K., Zeeman, M., Michna, P., Zingg, A., Buchmann, N., & Emmenegger, L. (2007). Methodical study of nitrous oxide eddy covariance measurements using quantum cascade laser spectrometery over a Swiss forest. Biogeosciences, 4(5), 927-939. doi:10.5194/bg-4-927-2007

Fernandez, I. J., Lawrence, G. B., & Son, Y. (1995). Soil-solution chemistry in a low-elevation spruce-fir ecosystem, Howland, Maine. Water, Air, and Soil Pollution, 84(1), 129-145. doi:10.1007/bf00479593

Fernandez, I. J., Rustad, L. E., & Lawrence, G. B. (1993). Estimating total soil mass, nutrient content, and trace metals in soils under a low elevation spruce-fir forest. Canadian Journal of Soil Science, 73(3), 317-328. doi:10.4141/cjss93-034

Flechard, C. R., Neftel, A., Jocher, M., Ammann, C., & Fuhrer, J. (2005). Bi-directional soil/atmosphere N2O exchange over two mown grassland systems with contrasting management practices. Global Change Biology, 11(12), 2114-2127. doi:doi:10.1111/j.1365-2486.2005.01056.x

Firestone, M. K., & Davidson, E. A. (1989). Microbiological basis of NO and N2O production and consumption in soil. In: Andreae, M.O., & Schimel, D. S. (eds.). Exchange *of trace gases between terrestrial ecosystems and the atmosphere*, pp.7-21. John Wiley & Sons, Inc., New York.

Goldberg, S. D., & Gebauer, G. (2009). Drought turns a Central European Norway spruce forest soil from an N2O source to a transient N2O sink. *Global Change Biology, 15*(4), 850-860.

Groffman, P. M. (2012). Terrestrial denitrification: challenges and opportunities. Ecological Processes, 1(1), 11. doi:10.1186/2192-1709-1-11

Groffman, P. M., Butterbach-Bahl, K., Fulweiler, R. W., Gold, A. J., Morse, J. L., Stander, E. K., . . . Vidon, P. (2009). Challenges to incorporating spatially and temporally explicit phenomena (hotspots and hot moments) in denitrification models. Biogeochemistry, 93(1), 49-77. doi:10.1007/s10533-008-9277-5

Hayatsu, M., Tago, K., & Saito, M. (2008). Various players in the nitrogen cycle: Diversity and functions of the microorganisms involved in nitrification and denitrification. Soil Science and Plant Nutrition, 54(1), 33-45. doi:10.1111/j.1747-0765.2007.00195.x

Holtan-Hartwig, L., Dörsch, P., & Bakken, L. R. (2002). Low temperature control of soil denitrifying communities: kinetics of N2O production and reduction. Soil Biology and Biochemistry, 34(11), 1797-1806. doi:https://doi.org/10.1016/S0038-0717(02)00169-4

Hursh, A., Ballantyne, A., Cooper, L., Maneta, M., Kimball, J., & Watts, J. (2017). The sensitivity of soil respiration to soil temperature, moisture, and carbon supply at the global scale. Global Change Biology, 23(5), 2090-2103.

IPCC (2014). *Climate Change 2014: Synthesis Report. Contribution of Working Groups I, II and III to the Fifth Assessment Report of the Intergovernmental Panel on Climate Change* [Core Writing Team, R.K. Pachauri and L.A. Meyer (eds.)]. IPCC, Geneva, Switzerland, 151 pp.

Jensen, B. B., & Burris, R. H. (1986). Nitrous oxide as a substrate and as a competitive inhibitor of nitrogenase. Biochemistry, 25(5), 1083-1088.

Keiluweit, M., Gee, K., Denney, A., & Fendorf, S. (2018). Anoxic microsites in upland soils dominantly controlled by clay content. *Soil Biology and Biochemistry, 118*, 42-50.

Keenan, T. F., Carbone, M. S., Reichstein, M., & Richardson, A. D. (2011). The model–data fusion pitfall: assuming certainty in an uncertain world. Oecologia, 167(3), 587. doi:10.1007/s00442-011-2106-x

Keller M, Matson PA (1994) Biosphere–atmosphere exchanges of trace gases in the tropics: evaluating the effects of land use changes. In: Global Atmospheric Biospheric Chemistry (ed. Prinn RG), pp. 103–117. Plenum Press, New York, NY.

Körner, H., & Zumft, W. G. (1989). Expression of denitrification enzymes in response to the dissolved oxygen level and respiratory substrate in continuous culture of Pseudomonas stutzeri. Applied and Environmental Microbiology, 55(7), 1670-1676.

Lamboni, M., Makowski, D., Lehuger, S., Gabrielle, B., & Monod, H. (2009). Multivariate global sensitivity analysis for dynamic crop models. Field Crops Research, 113(3), 312-320. doi:https://doi.org/10.1016/j.fcr.2009.06.007

Lindgren, F., & Rue, H. (2015). Bayesian spatial modelling with R-INLA. Journal of Statistical Software, 63(19), 1-25.

Linn, D. M., & Doran, J. W. (1984). Effect of water-filled pore space on carbon dioxide and nitrous oxide production in tilled and nontilled soils 1. *Soil Science Society of America Journal, 48*(6), 1267-1272.

Lloyd, J., & Taylor, J. A. (1994). On the Temperature Dependence of Soil Respiration. *Functional Ecology, 8*(3), 315-323. doi:10.2307/2389824

Lurndahl, N. (2016). Temporal and Spatial Trends in the Abundance of Functional Denitrification Genes and Observed Soil Moisture and Potential Denitrification Rates. MS, University of Minnesota, Minneapolis.

Metivier, K. A., Pattey, E., & Grant, R. F. (2009). Using the ecosys mathematical model to simulate temporal variability of nitrous oxide emissions from a fertilized agricultural soil. Soil Biology and Biochemistry, 41(12), 2370-2386. doi:https://doi.org/10.1016/j.soilbio.2009.03.007

Millington, R. J., & Shearer, R. C. (1971). Diffusion in aggregated porous media. Soil Science, 111(6), 372-378.

Morse, J. L., & Bernhardt, E. S. (2013). Using 15N tracers to estimate N2O and N2 emissions from nitrification and denitrification in coastal plain wetlands under contrasting land-uses. Soil Biology and Biochemistry, 57, 635-643. doi:https://doi.org/10.1016/j.soilbio.2012.07.025

Moyano, F. E., Manzoni, S., & Chenu, C. (2013). Responses of soil heterotrophic respiration to moisture availability: An exploration of processes and models. Soil Biology and Biochemistry, 59, 72-85.

Müller, C., Rütting, T., Kattge, J., Laughlin, R. J., & Stevens, R. J. (2007). Estimation of parameters in complex 15N tracing models by Monte Carlo sampling. Soil Biology and Biochemistry, 39(3), 715-726. doi:https://doi.org/10.1016/j.soilbio.2006.09.021

Myrgiotis, V., Williams, M., Topp, C. F., & Rees, R. M. (2018). Improving model prediction of soil N2O emissions through Bayesian calibration. Science of the total environment, 624, 1467-1477.

Myrold, D. D., & Tiedje, J. M. (1986). Simultaneous estimation of several nitrogen cycle rates using 15N: Theory and application. Soil Biology and Biochemistry, 18(6), 559-568. doi:https://doi.org/10.1016/0038-0717(86)90076-3

Nedwell, D. B., & Watson, A. (1995). CH4 production, oxidation and emission in a U.K. ombrotrophic peat bog: Influence of SO42− from acid rain. Soil Biology and Biochemistry, 27(7), 893-903. doi:https://doi.org/10.1016/0038-0717(95)00018-A

Omlin, M., Brun, R., & Reichert, P. (2001). Biogeochemical model of Lake Zürich: sensitivity, identifiability and uncertainty analysis. Ecological Modelling, 141(1), 105-123. doi:https://doi.org/10.1016/S0304-3800(01)00257-5

Or, D. (2019). The tyranny of small scales – on representing soil processes in global land surface models. Water Resources Research, 0(ja). doi:10.1029/2019wr024846

Parkin, T. B. (1987). Soil Microsites as a Source of Denitrification Variability1. Soil Science Society of America Journal, 51(5), 1194-1199. doi:10.2136/sssaj1987.03615995005100050019x

Parkin, T. B. (1993). Spatial Variability of Microbial Processes in Soil—A Review. Journal of Environmental Quality, 22(3), 409-417. doi:10.2134/jeq1993.00472425002200030004x

Potter, C. S., Matson, P. A., Vitousek, P. M., & Davidson, E. A. (1996). Process modeling of controls on nitrogen trace gas emissions from soils worldwide. Journal of Geophysical Research: Atmospheres, 101(D1), 1361-1377. doi:10.1029/95jd02028

R Core Team. (2018). R: A language and environment for statistical computing. R Foundation for Statistical Computing, Vienna, Austria. URL: https://www.R-project.org/

Resurreccion, A. C., Moldrup, P., Kawamoto, K., Hamamoto, S., Rolston, D. E., & Komatsu, T. (2010). Hierarchical, Bimodal Model for Gas Diffusivity in Aggregated, Unsaturated Soils. Soil Science Society of America Journal, 74(2), 481-491. doi:10.2136/sssaj2009.0055

Revolution Analytics & Weston, S. (2015). doParallel: Foreach Parallel Adaptor for the 'parallel' Package. R package version 1.0.10. https://CRAN.R-project.org/package=doParallel

Richardson, A. D., Hollinger, D. Y., Shoemaker, J. K., Hughes, H., Savage, K., & Davidson, E. A. (2019). Six years of ecosystem-atmosphere greenhouse gas fluxes measured in a sub-boreal forest. Scientific Data, 6(1), 117.

Richardson, A. D., Williams, M., Hollinger, D. Y., Moore, D. J. P., Dail, D. B., Davidson, E. A.,

. . . Savage, K. (2010). Estimating parameters of a forest ecosystem C model with measurements of stocks and fluxes as joint constraints. Oecologia, 164(1), 25-40. doi:10.1007/s00442-010-1628-y

Rue, H., Martino, S., & Chopin, N. (2009). Approximate Bayesian inference for latent Gaussian models by using integrated nested Laplace approximations. Journal of the Royal Statistical Society: Series B (Statistical Methodology), 71(2), 319-392. doi:doi:10.1111/j.1467-9868.2008.00700.x

Saha, D., Kemanian, A. R., Montes, F., Gall, H., Adler, P. R., & Rau, B. M. (2018). Lorenz Curve and Gini Coefficient Reveal Hot Spots and Hot Moments for Nitrous Oxide Emissions. Journal of Geophysical Research: Biogeosciences, 123(1), 193-206. doi:doi:10.1002/2017JG004041

Savage, K. E., & Davidson, E. A. (2003). A comparison of manual and automated systems for soil CO2 flux measurements: trade-offs between spatial and temporal resolution. Journal of Experimental Botany, 54(384), 891-899. doi:10.1093/jxb/erg121

Savage, K. E., Davidson, E. A., Abramoff, R. Z., Finzi, A. C., & Giasson, M.-A. (2018). Partitioning soil respiration: quantifying the artifacts of the trenching method. Biogeochemistry, 140(1), 53-63. doi:10.1007/s10533-018-0472-8

Savage, K. E., Davidson, E. A., & Richardson, A. D. (2008). A conceptual and practical approach to data quality and analysis procedures for high-frequency soil respiration measurements. Functional Ecology, 22(6), 1000-1007. doi:doi:10.1111/j.1365-2435.2008.01414.x

Savage, K. E., Phillips, R., & Davidson, E. (2014). High temporal frequency measurements of greenhouse gas emissions from soils. *Biogeosciences, 11*(10), 2709-2720. doi:10.5194/bg-11-2709-2014

Schlesinger, W. H. (2013). An estimate of the global sink for nitrous oxide in soils. *Global Change Biology, 19*(10), 2929-2931.

Shoun, H., Kim, D.-H., Uchiyama, H., & Sugiyama, J. (1992). Denitrification by fungi. FEMS Microbiology Letters, 94(3), 277-281. doi:10.1111/j.1574-6968.1992.tb05331.x

Sihi, D., Davidson, E. A., Chen, M., Savage, K. E., Richardson, A. D., Keenan, T. F., & Hollinger, D. Y. (2018). Merging a mechanistic enzymatic model of soil heterotrophic respiration into an ecosystem model in two AmeriFlux sites of northeastern USA. *Agricultural and Forest Meteorology, 252*, 155-166. doi:https://doi.org/10.1016/j.agrformet.2018.01.026

Silver, W. L., Lugo, A. E., & Keller, M. (1999). Soil oxygen availability and biogeochemistry along rainfall and topographic gradients in upland wet tropical forest soils. Biogeochemistry, 44(3), 301-328. doi:10.1007/bf00996995

Soetaert, K. (2016). R Package FME: Inverse modelling, sensitivity. Monte Carlo—Applied to a dynamic simulation model, (CRAN Vignette 2).[Availavle at https://cran. r-project. org/web/packages/FME/vignettes/FMEdyna. pdf.].

Soetaert, K., & Petzoldt, T. (2010). Inverse modelling, sensitivity and monte carlo analysis in R using package FME. Journal of Statistical Software, 33(3), 1-28.

Stark, J. M. (1996). Modeling the temperature response of nitrification. *Biogeochemistry, 35*(3), 433-445.

Stark, J. M., & Firestone, M. K. (1996). Kinetic characteristics of ammonium-oxidizer communities in a California oak woodland-annual grassland. Soil Biology and Biochemistry, 28(10-11), 1307-1317.

Stoyan, H., De-Polli, H., Böhm, S., Robertson, G. P., & Paul, E. A. (2000). Spatial heterogeneity of soil respiration and related properties at the plant scale. Plant and Soil, 222(1), 203-214. doi:10.1023/a:1004757405147

Syakila, A., Kroeze, C., & Slomp, C. P. (2010). Neglecting sinks for N_2O at the earth's surface: does it matter? *Journal of Integrative Environmental Sciences, 7*(S1), 79-87.

Teh, Y. A., Silver, W. L., & Conrad, M. E. (2005). Oxygen effects on methane production and oxidation in humid tropical forest soils. Global Change Biology, 11(8), 1283-1297. doi:doi:10.1111/j.1365-2486.2005.00983.x

Tian, H., Yang, J., Xu, R., Lu, C., Canadell, J. G., Davidson, E. A., . . . Zhang, B. (2019). Global soil nitrous oxide emissions since the preindustrial era estimated by an ensemble of terrestrial biosphere models: Magnitude, attribution, and uncertainty. Global Change Biology, 25(2), 640-659. doi:doi:10.1111/gcb.14514

Urmann, K., Gonzalez-Gil, G., Schroth, M. H., Hofer, M., & Zeyer, J. (2005). New field method: Gas push− pull test for the in-situ quantification of microbial activities in the vadose zone. Environmental Science & Technology, 39(1), 304-310.

Van't Hoff, J.H., Lehfeldt, R.A. (1899). *Lectures on theoretical and physical chemistry. Part 1. Chemical Dynamics*. Edward Arnold, London.

Verchot, L. V., Davidson, E. A., Cattânio, J. H., & Ackerman, I. L. (2000). Land-Use Change and Biogeochemical Controls of Methane Fluxes in Soils of Eastern Amazonia. Ecosystems, 3(1), 41-56. doi:10.1007/s100210000009

Verstraete, W., & Focht, D. (1977). Biochemical ecology of nitrification and denitrification. In Advances in microbial ecology (pp. 135-214): Springer.

Vieten, B. (2008). N_2O reduction in soils. PhD, University of Basel, Switzerland.

Wang, B., Brewer, P. E., Shugart, H. H., Lerdau, M. T., & Allison, S. D. (2019). Soil aggregates as biogeochemical reactors and implications for soil–atmosphere exchange of greenhouse gases—A concept. Global Change Biology, 25(2), 373-385. doi:doi:10.1111/gcb.14515

Wen, Y., Chen, Z., Dannenmann, M., Carminati, A., Willibald, G., Kiese, R., . . . Corre, M. D. (2016). Disentangling gross N2O production and consumption in soil. Scientific Reports, 6, 36517. doi:10.1038/srep36517 https://www.nature.com/articles/srep36517#supplementary-information Wood, S. N. (2017). Generalized additive models: an introduction with R: CRC press.

Westermann, P. (1993). Temperature regulation of methanogenesis in wetlands. Chemosphere, 26(1-4), 321-328.

Xu, X., Yuan, F., Hanson, P. J., Wullschleger, S. D., Thornton, P. E., Riley, W. J., . . . Tian, H. (2016). Reviews and syntheses: Four decades of modeling methane cycling in terrestrial ecosystems. Biogeosciences, 13(12), 3735-3755. doi:10.5194/bg-13-3735-2016

Yamulki, S., Goulding, K. W. T., Webster, C. P., & Harrison, R. M. (1995). Studies on no and N20 fluxes from a wheat field. Atmospheric Environment, 29(14), 1627-1635. doi:https://doi.org/10.1016/1352-2310(95)00059-8

Yan, Z., Liu, C., Todd-Brown, K. E., Liu, Y., Bond-Lamberty, B., & Bailey, V. L. (2016). Pore-scale investigation on the response of heterotrophic respiration to moisture conditions in heterogeneous soils. Biogeochemistry, 131(1), 121-134. doi:10.1007/s10533-016-0270-0

Yamazaki, T., Yoshida, N., Wada, E., & Matsuo, S. (1987). N_2O Reduction by Azotobacter vinelandii with Emphasis on Kinetic Nitrogen Isotope Effects. Plant and Cell Physiology, 28(2), 263-271. doi:10.1093/oxfordjournals.pcp.a077292

Yang, W. H., McNicol, G., Teh, Y. A., Estera-Molina, K., Wood, T. E., & Silver, W. L. (2017). Evaluating the Classical Versus an Emerging Conceptual Model of Peatland Methane Dynamics. Global Biogeochemical Cycles, 31(9), 1435-1453. doi:doi:10.1002/2017GB005622

Yoshida, N., Matsuo, S., Yamazaki, T., & Wada, E. (1987). N2O Reduction by Azotobacter vinelandii with Emphasis on Kinetic Nitrogen Isotope Effects. Plant and Cell Physiology, 28(2), 263-271. doi:10.1093/oxfordjournals.pcp.a077292

Zarnetske, J. P., Haggerty, R., Wondzell, S. M., Bokil, V. A., & González-Pinzón, R. (2012). Coupled transport and reaction kinetics control the nitrate source-sink function of hyporheic zones. Water Resources Research, 48(11). doi:doi:10.1029/2012WR011894

Zheng, J., & Doskey, P. V. (2015). Modeling Nitrous Oxide Production and Reduction in Soil through Explicit Representation of Denitrification Enzyme Kinetics. Environmental Science & Technology, 49(4), 2132-2139. doi:10.1021/es504513v